

# Study of $CP$ violation in $\Lambda_b^0 \rightarrow N^* M$ decays with the final-state rescattering mechanism

Hui-Qiang Shang<sup>a\*</sup>, Tian-Liang Feng<sup>b†</sup>, Jing Gao<sup>c‡</sup>, Qin Qin<sup>a§</sup> and Fu-Sheng Yu<sup>b¶</sup>

<sup>a</sup> *School of Physics, Huazhong University of Science and Technology, Wuhan 430074, China*

<sup>b</sup> *Frontiers Science Center for Rare Isotopes and School of Nuclear Science and Technology, Lanzhou University, Lanzhou 730000, China*

<sup>c</sup> *Helmholtz-Institut für Strahlen- und Kernphysik and Bethe Center for Theoretical Physics, Universität Bonn, D-53115 Bonn, Germany*

## Abstract

In this work, we investigate the charmless non-leptonic two-body  $\Lambda_b$  decays within the framework of final-state rescattering mechanism. In contrast to the Cutkosky cutting method, we compute both the absorptive and dispersive parts of the hadronic rescattering triangle diagrams. Based on the established formalism, we analyze the  $\Lambda_b \rightarrow N^*(1535, 1520) M$  decay processes with  $M = K_S, K_0^*(700), f_0(500, 980), \rho(770), \bar{K}^{*0}, \phi$ , and predict various physical observables, such as their branching ratios, direct and partial-wave  $CP$  asymmetries, as well as decay asymmetry parameters. These two-body decay processes are expected to contribute primarily to the subsequent four-body decay channels, such as  $\Lambda_b^0 \rightarrow p \pi^- \pi^+ \pi^-$ , whose  $CP$  asymmetry measurements will be accessible at the LHCb experiment.

## 1 Introduction

$CP$  violation plays a crucial role in understanding the matter–antimatter asymmetry in the universe [1], testing the validity of the Standard Model (SM), and probing possible new physics beyond the SM. In the SM,  $CP$  violation is explained through the well-known quark mixing mechanism, originally proposed by the Kobayashi and Maskawa, which is attributed to the complex phase in the Cabibbo-Kobayashi-Maskawa (CKM) matrix [2, 3]. However, compared to the observed baryon asymmetry in the universe [4], the  $CP$  violation predicted by the SM is far too small. This phenomenon strongly indicates that additional sources of  $CP$  violation beyond SM are required.

The CKM mechanism has been firmly validated in meson systems. The first experimental discovery of  $CP$  violation was observed in  $K$  meson decays [5–7]. Subsequently,

\*she@hust.edu.cn

†fengl18@lzu.edu.cn

‡gao@hiskp.uni-bonn.de

§qinq@hust.edu.cn

¶yufsh@lzu.edu.cn

$CP$ -violating effects were identified in  $B$  and  $D$  meson decays [8–13], thus further corroborating the validity of the theory. Recently, the LHCb collaboration has reported the first observation of the significant  $CP$  violation in  $\Lambda_b^0 \rightarrow p\pi^+K^-\pi^-$  decay channel [14], and the measured  $CP$  asymmetry is given by

$$\mathcal{A}_{CP} = \frac{\Gamma - \bar{\Gamma}}{\Gamma + \bar{\Gamma}} = (2.45 \pm 0.46 \pm 0.10)\% , \quad (1)$$

where  $\Gamma$  and  $\bar{\Gamma}$  denote the decay width of the  $\Lambda_b^0 \rightarrow p\pi^+K^-\pi^-$  process and its  $CP$ -conjugate process, respectively. This is the first time that LHCb collaboration reported the definitive observation of  $CP$  violation in baryon decays, confirming a long-sought phenomenon in particle physics. This breakthrough result represents a pivotal advancement in elucidating fundamental symmetry-breaking mechanisms and provides a new platform for testing the SM predictions and probing new physics beyond the SM.

In this work, we conduct a detailed investigation of charmless two-body non-leptonic  $\Lambda_b^0$  decays within the theoretical framework of the final-state rescattering mechanism [15], wherein the hadronic triangle loop integrals are systematically incorporated. This approach, which has been successfully applied to the  $\Lambda_c^+ \rightarrow \mathcal{B}V$  decays in an previous study [16], provides an appropriate treatment of non-perturbative long-distance effects. The rescattering mechanism is formulated as follows: the  $\Lambda_b^0$  first undergoes a short-distance weak decay into an intermediate baryon-meson pair, which subsequently rescatter via the exchange of another hadron. The rescattering, which is governed by strong interactions, is expected to capture the long-distance contribution. By explicitly separating the short- and long-distance dynamics, the computation avoids the double counting, ensuring a reliable and theoretically controlled description of the full amplitude. Both the absorptive (imaginary) and dispersive (real) parts of the triangle diagram amplitudes are included in the analysis, thereby enabling a comprehensive treatment of the interference between strong and weak phases that underlie  $CP$ -violating observables. Our analysis focuses on a class of decay channels including  $\Lambda_b^0 \rightarrow N^*(1535, 1520)M$  with  $M = K_S^0, K_0^*(700), f_0(500, 980), \rho^0, \bar{K}^{*0}, \phi$ . For these processes, we provide theoretical predictions for several physical observables, including branching ratios, direct and partial wave  $CP$  asymmetries. Furthermore, we also evaluate the decay asymmetry parameters, which serve as sensitive probes of spin correlations between involved particles and parity-violating effects in the processes.

The structure of this paper is as follows. In Section 2, we provide a concise overview of the theoretical framework employed in this work, including the naive factorization hypothesis, the quark-level topological diagram approach, and the final-state rescattering mechanism. The fundamental input parameters and numerical results are displayed in Section 3. In Section 4, we give a brief summary of this work and an outlook for future studies. The effective Lagrangians, the corresponding strong interaction vertices, and relevant expressions of the triangle diagrams and amplitudes are collected in the appendices.

## 2 Theoretical Framework

In this section, we introduce the theoretical framework that is used to calculate the amplitudes of charmless two-body non-leptonic  $\Lambda_b^0$  decays. Based on the weak effective Hamiltonian, the topological diagrams at partonic level for each decay channel are

obtained. The naive factorization hypothesis is adopted to evaluate the short-distance hadronic matrix elements, and the rescattering mechanism is employed to address the long-distance final-state interactions.

## 2.1 The effective Hamiltonian and short-distance contributions

The charmless two-body non-leptonic  $\Lambda_b^0$  decay processes involve at least three distinct scales:  $m_W \gg m_b \gg \Lambda_{\text{QCD}}$ . To systematically account for the physics at different scales, it is advantageous to employ the effective field theory. By integrating out the heavy degrees of freedom associated with the electroweak scale (e.g., the  $W$  boson) and performing the operator product expansion, we obtain an effective weak Hamiltonian that governs  $b$ -quark decays at the scale  $\mu = m_b$ . Therefore, all the short-distance contributions above the scale  $m_b$  are encapsulated in the Wilson coefficients, which are perturbatively calculable and independent of the specific hadronic initial and final states. Moreover, the non-perturbative long-distance effects are encoded in the hadronic matrix elements of local operators. The effective weak Hamiltonian for the  $b \rightarrow u$  transition at tree level and the  $b \rightarrow q$  transition ( $q = d, s$ ) at loop level takes the form [17, 18]:

$$\mathcal{H}_{\text{eff}} = \frac{G_F}{\sqrt{2}} \{ V_{ub} V_{uq}^* [C_1(\mu) O_1(\mu) + C_2(\mu) O_2(\mu)] - V_{tb} V_{tq}^* [\sum_{i=3}^{10} C_i(\mu) O_i(\mu)] \} + \text{h.c.} , \quad (2)$$

where  $G_F$  is the Fermi coupling constant,  $V_{ij}$  are the elements of the CKM matrix,  $C_i(\mu)$  are the Wilson coefficients evaluated at the renormalization scale  $\mu$ , and  $O_i(\mu)$  denote the corresponding local four-quark operators. The explicit forms of  $O_i(\mu)$  and the numerical values of  $C_i(\mu)$  can be found in [18]. Thus, the charmless two-body non-leptonic  $\Lambda_b^0$  decay amplitudes are determined by the hadronic matrix elements of the corresponding local four-quark operators

$$\langle M \mathcal{B} | \mathcal{H}_{\text{eff}} | \Lambda_b^0(p_i) \rangle = \frac{G_F}{\sqrt{2}} V_{\text{CKM}} \sum_i C_i \langle \mathcal{B} M | O_i | \Lambda_b^0 \rangle , \quad (3)$$

where  $M$  and  $\mathcal{B}$  denote the meson and baryon in the final state, respectively, and  $V_{\text{CKM}}$  stands for the relevant combination of CKM matrix elements. For the tree operators of the decay processes, the involved combinations of the Wilson coefficients are  $a_1(\mu) = C_1(\mu) + C_2(\mu)/3 = 1.03$  and  $a_2(\mu) = C_2(\mu) + C_1(\mu)/3 = 0.103$  at  $\mu = m_b$ , respectively [18]. For penguin operators, we take  $a_3(\mu) = C_3(\mu) + C_4(\mu)/3 = 3.6 \times 10^{-3}$ ,  $a_4(\mu) = C_3(\mu)/3 + C_4(\mu) = 2.3 \times 10^{-2}$ ,  $a_5(\mu) = C_5(\mu) + C_6(\mu)/3 = -2.29 \times 10^{-3}$  and  $a_6(\mu) = C_5(\mu)/3 + C_6(\mu) = -29.8 \times 10^{-3}$  at  $\mu = m_b$ ,  $a_7(\mu) = C_7(\mu) + C_8(\mu)/3 = 12.2 \times 10^{-4}$ ,  $a_8(\mu) = C_7(\mu)/3 + C_8(\mu) = 7.57 \times 10^{-4}$ ,  $a_9(\mu) = C_9(\mu) + C_{10}(\mu)/3 = -82.2 \times 10^{-4}$ ,  $a_{10}(\mu) = C_9(\mu)/3 + C_{10}(\mu) = -8.20 \times 10^{-4}$  at  $\mu = m_b$  [18].

With the aid of the naive factorization hypothesis [19], the hadronic matrix elements can be approximated as a product of two separate matrix elements

$$\langle \mathcal{B} M | O_i | \Lambda_b^0 \rangle \rightarrow \langle M | J_{i,1} | 0 \rangle \otimes \langle \mathcal{B} | J_{i,2} | \Lambda_b^0 \rangle . \quad (4)$$

For instance, when  $O_i = O_{1,2}$ ,  $J_{i,1}$  and  $J_{i,2}$  correspond to the  $V - A$  currents with the quark flavor transitions. The matrix elements  $\langle M | J_{i,1} | 0 \rangle$  and  $\langle \mathcal{B} | J_{i,2} | \Lambda_b^0 \rangle$  are parametrized by the decay constants of the emitted mesons and the heavy-to-light form factors of the  $\Lambda_b^0 \rightarrow \mathcal{B}$  transitions. This factorization method allows for tractable calculations, although it neglects certain non-factorizable effects. The amplitudes of charmless two-body non-leptonic  $\Lambda_b^0$  decays take the following forms,

- for the final states are pseudoscalar or scalar mesons,

$$\mathcal{A}(\Lambda_b^0(p_i) \rightarrow \mathcal{B}(p_4)P/S) = i\bar{u}(p_4)[A + B\gamma_5]u(p_i) ; \quad (5)$$

- for the final states are vector mesons,

$$\mathcal{A}(\Lambda_b^0(p_i) \rightarrow \mathcal{B}(p_4)V) = \bar{u}(p_4)[A_1\gamma_\mu\gamma_5 + A_2\frac{p_{f,\mu}}{m_i}\gamma_5 + B_1\gamma_\mu + B_2\frac{p_{f,\mu}}{m_i}]\epsilon^{*\mu}u(p_i) , \quad (6)$$

where  $u(p_i)$  and  $u(p_4)$  denote the Dirac spinors of the initial and final baryons, respectively, and  $\epsilon^{*\mu}$  is the polarization of the final-state vector meson [20, 21]. The invariant amplitudes  $A$ ,  $B$ ,  $A_i$ , and  $B_i$  ( $i = 1, 2$ ) are the combinations of the the Wilson coefficients, the decay constants, and the heavy-to-light transition form factors, which encode the dynamics of the underlying hadronic transition. Detailed definitions and phenomenological discussions of these invariant amplitudes can be found in Refs. [20–22]. It is worth emphasizing that short-distance contributions not only encode the effects of high-scale physics but also play a crucial role in shaping the long-distance hadronic dynamics, as will be further illustrated in the subsequent discussion.

## 2.2 Long-distance contributions within the framework of rescattering mechanism

In charmless two-body non-leptonic  $\Lambda_b^0$  decay processes, long-distance contributions are of substantial significance, particularly for the prediction of the relative strong phases and subsequently for the  $CP$  asymmetries. The final-state rescattering mechanism offers a theoretically well-founded and physically transparent framework for characterizing long-distance contributions in  $\Lambda_b$  decays. Based on  $CPT$  invariance and unitarity, Wolfenstein and Suzuki proposed a formalism for final-state interactions at the hadronic level [23, 24]. Subsequently, Cheng, Chua, and Soni performed a systematic study of two-body B meson decays, including the effects of final-state interactions [25]. In the time-evolution picture, short-distance interactions associated with weak decays occur promptly at early times, whereas long-distance rescattering effects emerge at later stages as the decay products propagate and interact. Thus, the full amplitude can be expressed as [26]

$$\mathcal{A}(\Lambda_b^0 \rightarrow f) = \sum_i \langle f | U(+\infty, \tau) | i \rangle \langle i | \mathcal{H}_{eff} | \Lambda_b^0 \rangle , \quad (7)$$

where the index  $i$  runs over all possible intermediate states to account for the complete rescattering contributions. The matrix element  $\langle i | \mathcal{H}_{eff} | \Lambda_b^0 \rangle$  does not generate strong phases, while the rescattering part  $\langle f | U(+\infty, \tau) | i \rangle$  introduces a complex amplitude with a nonzero phase. Since the long-distance contributions are intrinsically nonperturbative, they can be estimated at the hadronic level via a single-particle-exchange approximation. Thus, the long-distance contributions to the charmless two-body non-leptonic  $\Lambda_b^0$  decays are modeled via hadronic triangle diagrams, which corresponds to the rescattering process between two intermediate hadrons after the weak decay of the  $\Lambda_b^0$ , as illustrated in Fig. 1. Previous studies [27, 28] have shown that two-body scatterings dominate the final-state interactions, while the contributions from three-body and four-body intermediate states are relatively small. Therefore, we neglect these contributions in this work.

The diagrams in Fig. 1 effectively encode the final-state interactions and provide a natural mechanism for incorporating rescattering effects into the decay amplitudes. To

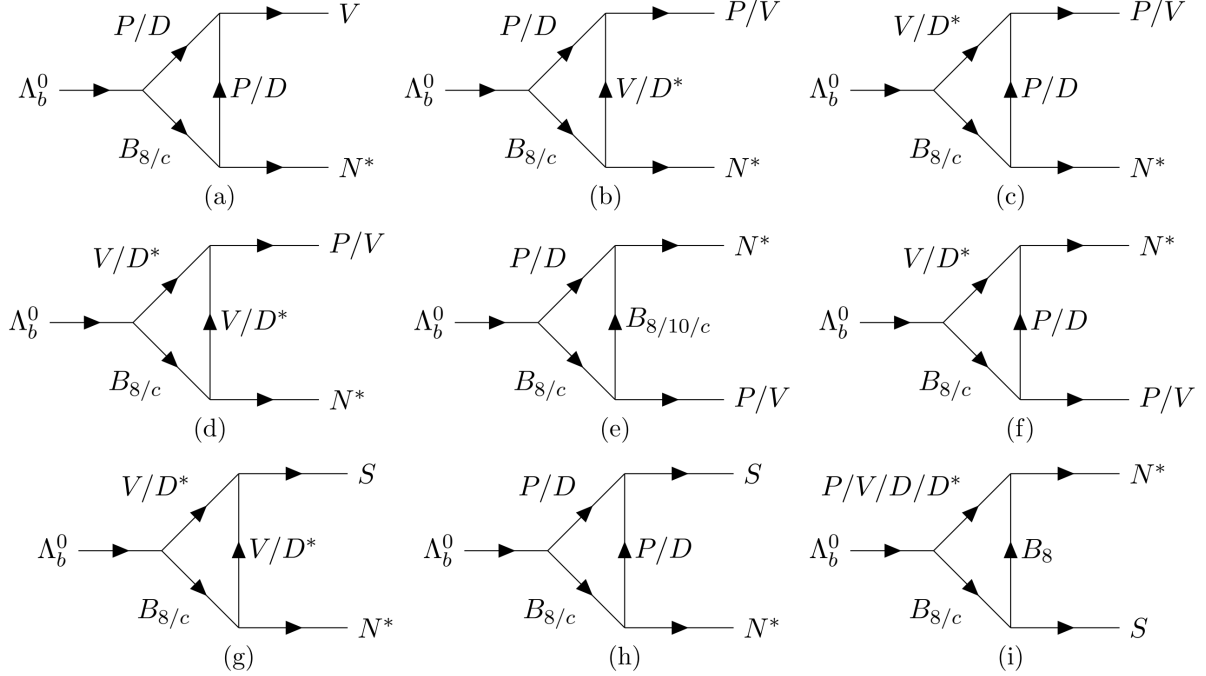


Figure 1: The diagrams of  $\Lambda_b^0 \rightarrow N^* M$  with  $M = K_S, K_0^*(700), f_0(500, 980), \rho(770), \bar{K}^{*0}, \phi$ , from rescattering mechanism at hadronic level with exchanging one single particle, where the  $B_8, B_c, B_{10}, N^*$  denote octet baryons, charmed baryons, decuplet baryons and  $N^*(1520, 1535)$ , respectively, and  $P, S, V, D$  and  $D^*$  are pseudoscalar, vector,  $D$  and  $D^*$  mesons, respectively.

evaluate these triangle diagrams, we need to combine the weak interaction vertex, treated as a short-distance amplitude under the naive factorization hypothesis, with the strong interaction vertices of the rescattering processes. The corresponding effective Lagrangian and Feynman rules for the strong interaction vertices are collected in Appendix A and Appendix B, respectively.

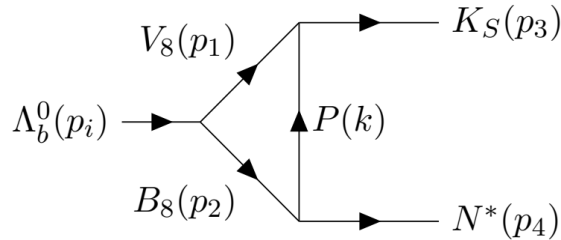


Figure 2: The diagram of  $\Lambda_b^0 \rightarrow N^* K_S$  with intermediate states octet vector meson  $V_8$  and octet baryons  $B_8$  rescattering by exchanging a pseudoscalar meson.

Employing the established Feynman rules of strong interaction vertices and the factorization formula of weak transition amplitudes, we can derive the analytical expressions for the triangle diagrams displayed in Fig. 1, by performing the relevant hadronic loop integrals. Then we give an example of the decay  $\Lambda_b^0 \rightarrow N^* K_S$ , with intermediate states an octet vector meson  $V_8(p_1)$  and an octet baryon  $B_8(p_2)$  rescattering by exchanging a pseudoscalar meson  $P(k)$ , as shown in Fig. 2. The final analytical expressions for the

$\Lambda_b^0 \rightarrow N^*(1520, 1535)K_S$  amplitudes are integrals of the loop momentum  $k$ ,

$$\begin{aligned} \mathcal{M}[V_8, B_8; P](1520) &= i^5 \int \frac{d^4 k}{(2\pi)^4} \frac{g_{VPP}}{\sqrt{2}} \frac{f_{\pi NN^*}^{1520}}{m_\pi} \bar{u}_\mu(p_4, s_4) \gamma_5 k^\mu (\not{p}_2 + m_2) [A_1 \gamma_\nu \gamma_5 + A_2 \frac{p_{2\nu}}{m_i} \gamma_5 \\ &\quad + B_1 \gamma_\nu + B_2 \frac{p_{2\nu}}{m_i}] \times u(p_i, s_i) \times (-g^{\nu\alpha} + \frac{p_1^\nu p_1^\alpha}{m_1^2})(p_3 + k)_\alpha \times \mathcal{F} \times \mathcal{P}, \\ \mathcal{M}[V_8, B_8; P](1535) &= -i^6 \int \frac{d^4 k}{(2\pi)^4} \frac{g_{VPP}}{\sqrt{2}} \frac{f_{\pi NN^*}^{1535}}{m_\pi} \bar{u}(p_4, s_4) \gamma_\mu k^\mu (\not{p}_2 + m_2) [A_1 \gamma_\nu \gamma_5 + A_2 \frac{p_{2\nu}}{m_i} \gamma_5 \\ &\quad + B_1 \gamma_\nu + B_2 \frac{p_{2\nu}}{m_i}] \times u(p_i, s_i) \times (-g^{\nu\alpha} + \frac{p_1^\nu p_1^\alpha}{m_1^2})(p_3 + k)_\alpha \times \mathcal{F} \times \mathcal{P}, \end{aligned} \quad (8)$$

where the  $f_{\pi NN^*}^{(1520, 1535)}$  and  $g_{VPP}$  denote the corresponding strong interaction vertices. And  $m_i$  are the mass of the initial state  $\Lambda_b^0$ .  $A_1, A_2, B_1, B_2$  encode the short-distance contributions. Besides,  $\mathcal{P}$  is the compact form of the product of the involved propagators,

$$\mathcal{P} = \frac{1}{p_1^2 - m_1^2 + i\epsilon} \cdot \frac{1}{p_2^2 - m_2^2 + i\epsilon} \cdot \frac{1}{k^2 - m_k^2 + i\epsilon}. \quad (9)$$

where  $p_1, p_2, k$  are the momenta of the three intermediate particles as shown in Fig. 2, and  $m_1, m_2, m_k$  are their masses, while  $\mathcal{F}$  is the regulator form factors for the exchange particles. The complete set of analytical expressions for all the triangle diagrams computed in this work are summarized in Appendix C and the full amplitudes of  $\Lambda_b \rightarrow N^* M$  with  $M = K_S, K_0^*(700), f_0(500, 980), \rho(770), \bar{K}^{*0}, \phi$ , are collected in Appendix D.

It should be noted that we introduce the regulator form factor  $\mathcal{F}$  in order to account for the off-shell effects of the intermediate particles, as well as the substructure effects of the exchange particles, and regularize the inevitable divergence appearing in the master integrals of the triangle diagrams. Here we adopt the following expression [29]

$$\mathcal{F}(\Lambda, k, m_k) = \frac{\Lambda^4}{(k^2 - m_k^2)^2 + \Lambda^4}, \quad (10)$$

where cutoff parameter  $\Lambda$  is introduced, basically working equivalently to the model parameter  $\eta$  in Ref. [16]. One single value of the model parameter  $\eta$  has been applied to the study of many decay channels, under the assumption that all intermediate particles are light and can be related through the SU(3) flavor symmetry. However, the situation is markedly different in the case of  $\Lambda_b^0$  decays, where charmed hadronic rescattering processes are involved and charm loop effects should be taken into consideration. Taking the decay  $\Lambda_b \rightarrow N^*(1535)K_S$  as an example, the initial particle  $\Lambda_b$  can decay into the final states  $N^*$  and  $K_S$  via two different intermediate states: one is through the intermediate states  $\{p, K^{*-}\}$  with a  $\pi^+$  exchange, and the other is through  $\{D_s^{*-}, \Lambda_c^+\}$  with a  $D^-$  exchange. The light mesons  $\{\pi, K^*\}$ , which belong to the pseudoscalar and vector meson octet, have very similar masses. Thus a single parameter suffices to describe these contributions based on approximate SU(3) flavor symmetry for light hadrons. In contrast, charmed mesons and baryons are significantly heavier, and their off-shell effects are substantially different, which necessitates the introduction of a separate model parameter to account for them. Therefore, we introduce two different parameters,  $\Lambda_{\text{charm}}$  and  $\Lambda_{\text{charmless}}$ , to distinguish them. The parameter  $\Lambda_{\text{charm}}$  is associated with charmed triangle diagrams, while  $\Lambda_{\text{charmless}}$  applies to the charmless ones. Both of them have been determined in a previous study of  $\Lambda_b^0 \rightarrow p\pi^-$  and  $\Lambda_b^0 \rightarrow pK^-$  [30].

### 3 Numerical results and analysis

In this section, we summarize the input parameters used for numerical calculations and present the results for the branching ratios, the asymmetry parameters, and the  $CP$  asymmetries of the following decay channels, categorized by the type of final state mesons:

- Pseudoscalar meson:  $\Lambda_b^0 \rightarrow N^*(1535, 1520)K_S^0$
- Scalar meson:  $\Lambda_b^0 \rightarrow N^*(1535, 1520)K_0^*(700)/f_0(500, 980)$
- Vector meson:  $\Lambda_b^0 \rightarrow N^*(1535, 1520)\rho^0/\bar{K}^{*0}/\phi$ .

#### 3.1 Basic inputs

In this work, all the masses of quarks and hadrons used as input parameters are taken from Ref. [31] and listed in Table. 1. The light quark masses correspond to the  $\overline{\text{MS}}$  masses evaluated at the renormalization scale  $\mu = 2$  GeV, and the heavy quark masses  $m_b$  and  $m_c$  are given in the  $\overline{\text{MS}}$  scheme at the scale of their respective  $\overline{\text{MS}}$  masses. The decay constants of the pseudoscalar and vector mesons are taken from Ref. [22] and summarized in Table. 2. The CKM matrix is expanded in the Wolfenstein parameterization as [2, 3]

$$V_{\text{CKM}} = \begin{pmatrix} V_{ud} & V_{us} & V_{ub} \\ V_{cd} & V_{cs} & V_{cb} \\ V_{td} & V_{ts} & V_{tb} \end{pmatrix} = \begin{pmatrix} 1 - \lambda_W^2/2 & \lambda_W & A\lambda_W^3(\rho - i\eta) \\ -\lambda_W & 1 - \lambda_W^2/2 & A\lambda_W^2 \\ A\lambda_W^3(1 - \rho - i\eta) & -A\lambda_W^2 & 1 \end{pmatrix} + \mathcal{O}(\lambda_W^4), \quad (11)$$

where the Wolfenstein parameters are taken as  $A = 0.823$ ,  $\rho = 0.141$ ,  $\eta = 0.349$ , and  $\lambda_W = 0.225$ . Here the subscript  $W$  is introduced to the parameter  $\lambda_W$  to distinguish it from the  $\lambda$  function used in Ref. [31].

Table 1: Masses of baryons, mesons, and quarks used in this work [31].

Parameters	$\Lambda_b$	$\Lambda_c^+$	$p$	$n$	$N^*(1520)$	$N^*(1535)$	$\Lambda^0$
Mass (GeV)	5.619	2.286	0.938	0.940	1.515	1.530	1.116
Parameters	$D^\pm$	$D^0$	$D^*$	$D_s$	$D_s^*$	$K$	$K^*$
Mass (GeV)	1.869	1.865	2.007	1.968	2.106	0.493	0.892
Parameters	$\rho$	$\pi$	$\omega$	$\phi$	$f_0(500)$	$f_0(980)$	
Mass (GeV)	0.770	0.140	0.783	1.020	0.513	0.980	
Parameters	$u$	$d$	$s$	$c$	$b$		
Mass (MeV)	2.16	4.70	93.5	1270	4180		

In calculation of the short distance contributions, the weak transition  $\Lambda_b \rightarrow p, n, \Lambda^0, \Lambda_c$  form factors serve as the essential hadronic input parameters and have been investigated within the various QCD-based theoretical methods, such as perturbative QCD approach [18], (covariant) light-front quark model [32, 33], QCD factorization [34], soft-collinear effective theory [35] and light cone sum rules [36]. In this work, we employ

Table 2: Decay constants of pseudoscalar and vector mesons used in this work [22].

Decay constant	$f_\pi$	$f_K$	$f_\rho$	$f_\omega$	$f_\phi$	$f_{K^*}$	$f_{D^*}$	$f_D$	$f_{D_s}$	$f_{D_s^*}$
Value [MeV]	130.3	155.5	216	187	215	210	230	212	250	271
Decay constant	$f_{J/\psi}$	$f_{\eta_c}$	$f_{\eta_u}$	$f_{\eta_d}$	$f_{\eta_s}$	$f_{\eta'_u}$	$f_{\eta'_d}$	$f_{\eta'_s}$		
Value [MeV]	418	387	54	54	-111	44	44	136		

Table 3: The values of the  $\Lambda_b \rightarrow p, n, \Lambda^0, \Lambda_c$  transition form factors from covariant light-front quark model [22]. The definitions of  $f_{1,2}$  and  $g_{1,2}$  can be found in [22].

Decay	$f_1(0)$	$f_2(0)$	$g_1(0)$	$g_2(0)$
$\Lambda_b \rightarrow \Lambda_c^+$	0.500	-0.098	0.509	-0.015
$\Lambda_b \rightarrow p$	0.128	-0.056	0.129	-0.033
$\Lambda_b \rightarrow \Lambda^0$	0.131	-0.048	0.132	-0.023
$\Lambda_b \rightarrow n$	0.128	-0.056	0.129	-0.033

the theoretical results for the heavy-to-light baryonic form factors obtained in Ref. [22], which are summarized in Table. 3.

In the long distance contribution, the strong coupling constants are the fundamental non-perturbative inputs. We adopt the values derived from light-cone sum rules, which take into account the  $SU(3)_f$  symmetry breaking effects [37, 38]. For the strong coupling constants involving the excited nucleon states  $N^*(1535, 1520)$ , the values are taken from Ref. [39]. The strong coupling constants for the excited nucleon states  $N^*(1535, 1520)$  and charmless mesons are

$$f_{\pi NN^*}^{1520} = -1.71, f_{\pi NN^*}^{1535} = 0.49, g_{\omega NN^*}^{1520} = 7.7, g_{\omega NN^*}^{1535} = -4.5, g_{\rho NN^*}^{1520} = 4.5, g_{\rho NN^*}^{1535} = -2.9. \quad (12)$$

The remaining strong coupling constants of this type involving charmed mesons are determined under the assumption of  $SU(4)$  flavor symmetry [40]. Furthermore, the strong couplings for two charmed mesons and one light meson are taken from Ref. [25]. The values are given by

$$g_{D^* D^* P_8} = \frac{g_{D^* D^* P_8}}{\sqrt{m_D m_{D^*}}}, \quad g_{DDV} = g_{D^* D^* V} = \frac{\beta g_V}{\sqrt{2}}, \quad f_{D^* DV} = \frac{f_{D^* D^* V}}{m_{D^*}} = \frac{\lambda g_V}{\sqrt{2}}, \quad (13)$$

where  $g_V = m_\rho/f_\pi$ ,  $\beta = 0.9$ ,  $\lambda = 0.56 \text{ GeV}^{-1}$  and  $g_{D^* D^* P_8} = 17.9$ .  $P_8$  denotes the octet pseudoscalar meson and  $g_{D^* D^* P_8}$  is extracted from the experimental data of the  $D^*$  decay width [25]. In addition, the strong coupling constants for charmed hadrons and light baryon octet are taken from Ref. [41]. These strong coupling constants are defined in the corresponding effective Lagrangians collected in Appendix A.

### 3.2 Branching ratios

We first calculate the decay widths of the decay channels. The expression for the decay width is obtained by summing the squares of all the helicity amplitudes over the spins of

the initial and final states, and averaging over the spin of the initial particle, as given by:

$$\Gamma(\Lambda_b \rightarrow N^* M) = \frac{p_c}{8\pi m_{\Lambda_b}^2} \frac{1}{2} \sum_{\lambda_i \lambda_f \lambda_M} |H_{\lambda_f, \lambda_M}^{\lambda_i}(\Lambda_b \rightarrow N^* M)|^2, \quad (14)$$

where  $p_c = \frac{1}{2m_{\Lambda_b}} \sqrt{[m_{\Lambda_b}^2 - (m_{N^*}^2 + m_M^2)][m_{\Lambda_b}^2 - (m_{N^*}^2 - m_M^2)]}$  is the momentum of  $N^*$  in the rest frame of  $\Lambda_b$ , and  $H$  denotes the helicity amplitudes with the indices  $\lambda_i$ ,  $\lambda_f$ , and  $\lambda_M$ , labelling the helicities of the initial-state baryon, the final-state baryon and the meson, respectively. Accordingly, the branching ratios are obtained by dividing the decay width of each channel by the total decay width of  $\Lambda_b$ .

Based on the above formulas, the input parameters, and the model parameters  $\Lambda_{\text{charm}} = 1.0 \pm 0.1$  and  $\Lambda_{\text{charmless}} = 0.5 \pm 0.1$ , the  $CP$ -averaged  $\Lambda_b \rightarrow N^* M$  branching ratios are evaluated, and the results are shown in Table. 4. The uncertainties arise from the uncertainties of the introduced model parameters. We do not consider the uncertainties induced by the variation of the scale  $\mu$ , because these uncertainties can be safely neglected in comparison with those induced by the model parameters.

We find that the branching ratio of the  $\Lambda_b \rightarrow N^*(1535)K_S$ , with the pseudoscalar meson in the final state, is of  $\mathcal{O}(10^{-5})$ , while the  $\Lambda_b \rightarrow N^*(1535)K_0^*(700)$  with the scalar meson in the final state is of  $\mathcal{O}(10^{-8})$ . Both of them are dominated by charm-loop triangle diagrams, but involve different charmed hadrons in the loops, as  $K_S$  and  $K_0^*(700)$  have different parities. For  $\Lambda_b \rightarrow N^*(1535)K_S$ , the loop contains the  $D^* \Lambda_c N^*$  vertex; while for  $\Lambda_b \rightarrow N^*(1535)K_0^*(700)$ , the loop contains the  $D \Lambda_c N^*$  vertex. From the corresponding Lagrangian (32) and the values for the couplings (12), it can be seen that the magnitude of the former is enhanced by the factors of  $m_{\Lambda_b}/m_D \sim 3$  and  $g_{VNN^*}/g_{PNN^*} \sim 6$ , and can thus account for the branching ratio hierarchy of nearly three orders of magnitude. In addition, as the  $SVV$  couplings are not available currently, we have neglected the involved contributions to  $\Lambda_b \rightarrow N^* K_0^*(700)$ . Therefore,  $\Lambda_b \rightarrow N^* K_0^*(700)$  and also the  $\Lambda_b \rightarrow N^* f_0(500, 980)$  channels, in which the final states involve a scalar meson, await the couplings to have more reliable predictions. Among the decay channels with a vector meson in the final state, the branching ratio of  $\Lambda_b \rightarrow N^*(1535)\phi$  is extremely small, which is due to the Okubo-Zweig-Iizuka suppression [42].

In the calculation of the triangle diagrams formulating long-distance dynamics, off-shell effects of all particles are taken into account and are characterized by the model parameters  $\Lambda_{\text{charmless}}$  and  $\Lambda_{\text{charm}}$ . To examine the dependence of the branching ratio on the parameters, we show the variation of the branching ratio for the channels  $\Lambda_b \rightarrow N^*(1535, 1520)K_S/\bar{K}^{*0}$  with respect to  $\Lambda_{\text{charmless}}$  and  $\Lambda_{\text{charm}}$  in Fig. 3. Taking the channel  $\Lambda_b \rightarrow N^* K_S$  as an example, this process is dominated by the tree amplitude proportional to  $V_{cb} V_{cs}^* a_1$  and the branching ratio exhibits the scaling of  $(\Lambda_{\text{charm}})^8$ . As the dominant contribution to the decay amplitude originates from the charmed triangle diagrams, which exceed charmless diagrams by approximately two to three orders of magnitude, the branching ratio is significantly more sensitive to the parameter  $\Lambda_{\text{charm}}$  than to  $\Lambda_{\text{charmless}}$ .

Apart from the model parameters, the decay branching ratio still depends on two additional input parameters, namely the heavy-to-light form factors and the strong coupling constants. These two parameters can be calculated using QCD-based theoretical methods or extracted from experimental data. In particular, for the couplings involving an excited nucleon  $N^*$ , a charmed baryon  $\Lambda_c$ , and a charmed meson  $D$ , we resort to  $SU(4)$  flavor symmetry to estimate the corresponding coupling constants [29], which

Table 4: Branching ratios and partial-wave branching ratios of  $\Lambda_b \rightarrow N^* M$ .

Decay channel	Br	Br <sup>S-wave</sup>	Br <sup>P-wave</sup>
$N^*(1535)K_S$	$(1.62^{+1.79}_{-0.91}) \times 10^{-5}$	$(0.10^{+0.11}_{-0.06}) \times 10^{-5}$	$(1.52^{+1.69}_{-0.85}) \times 10^{-5}$
$N^*(1535)K_0^*(700)$	$(3.16^{+0.42}_{-0.22}) \times 10^{-8}$	$(2.40^{+0.32}_{-0.17}) \times 10^{-8}$	$(0.76^{+0.33}_{-0.20}) \times 10^{-8}$
$N^*(1535)f_0(500)$	$(4.18^{+3.81}_{-1.91}) \times 10^{-7}$	$(3.03^{+2.74}_{-1.40}) \times 10^{-7}$	$(1.14^{+1.07}_{-0.51}) \times 10^{-7}$
$N^*(1535)f_0(980)$	$(1.55^{+1.76}_{-0.87}) \times 10^{-6}$	$(1.43^{+1.61}_{-0.81}) \times 10^{-6}$	$(0.12^{+0.15}_{-0.07}) \times 10^{-6}$
$N^*(1520)K_S$	$(7.17^{+8.01}_{-4.05}) \times 10^{-5}$	$(6.55^{+7.31}_{-3.69}) \times 10^{-5}$	$(0.62^{+0.70}_{-0.36}) \times 10^{-5}$
$N^*(1520)K_0^*(700)$	$(1.92^{+1.67}_{-0.90}) \times 10^{-7}$	$(1.91^{+1.64}_{-0.90}) \times 10^{-7}$	$1.65^{+3.32}_{-0.90} \times 10^{-9}$
$N^*(1520)f_0(500)$	$(6.09^{+1.95}_{-1.10}) \times 10^{-8}$	$(4.18^{+1.08}_{-0.73}) \times 10^{-8}$	$(1.91^{+0.91}_{-0.51}) \times 10^{-8}$
$N^*(1520)f_0(980)$	$(4.59^{+4.60}_{-2.37}) \times 10^{-7}$	$(3.18^{+3.14}_{-1.62}) \times 10^{-7}$	$(1.40^{+1.46}_{-0.74}) \times 10^{-8}$
$N^*(1535)\bar{K}^{*0}$	$(1.66^{+1.90}_{-0.95}) \times 10^{-4}$	—	—
$N^*(1535)\rho(770)$	$(0.85^{+0.56}_{-0.33}) \times 10^{-4}$	—	—
$N^*(1535)\phi$	$(1.89^{+5.69}_{-1.55}) \times 10^{-10}$	—	—
$N^*(1520)\bar{K}^{*0}$	$(1.58^{+1.69}_{-0.86}) \times 10^{-4}$	—	—
$N^*(1520)\rho(770)$	$(1.44^{+1.19}_{-0.61}) \times 10^{-4}$	—	—
$N^*(1520)\phi$	$(1.05^{+3.40}_{-0.87}) \times 10^{-9}$	—	—

will introduce additional sources of uncertainty. Thus, improving the precision of these strong couplings is essential for more reliable theoretical predictions and for a deeper understanding of the dynamics of charmless non-leptonic  $\Lambda_b$  decays.

### 3.3 $CP$ asymmetries

We are now ready to explore the  $CP$  asymmetries of the  $\Lambda_b \rightarrow N^* M$  channels. The global direct  $CP$  asymmetry for each channel is defined by

$$a_{CP}^{\text{dir}} = \frac{\Gamma - \bar{\Gamma}}{\Gamma + \bar{\Gamma}}, \quad (15)$$

where  $\bar{\Gamma}$  denotes the decay width of the corresponding  $CP$ -conjugate process  $\bar{\Lambda}_b \rightarrow \bar{N}^* \bar{M}$ . For understanding the contributions to the  $CP$  violation from different partial waves, we derive the partial wave amplitudes from helicity amplitudes for the  $\Lambda_b \rightarrow N^* P/S$  processes by [43]

$$H_{+1/2} = \frac{1}{\sqrt{2}}(S + P), \quad H_{-1/2} = \frac{1}{\sqrt{2}}(S - P). \quad (16)$$

Subsequently, we define the partial-wave  $CP$ -violating observables in  $\Lambda_b \rightarrow N^* P/S$  processes as [44]

$$a_{CP}^S = \frac{|S|^2 - |\bar{S}|^2}{|S|^2 + |\bar{S}|^2}, \quad a_{CP}^P = \frac{|P|^2 - |\bar{P}|^2}{|P|^2 + |\bar{P}|^2}, \quad (17)$$

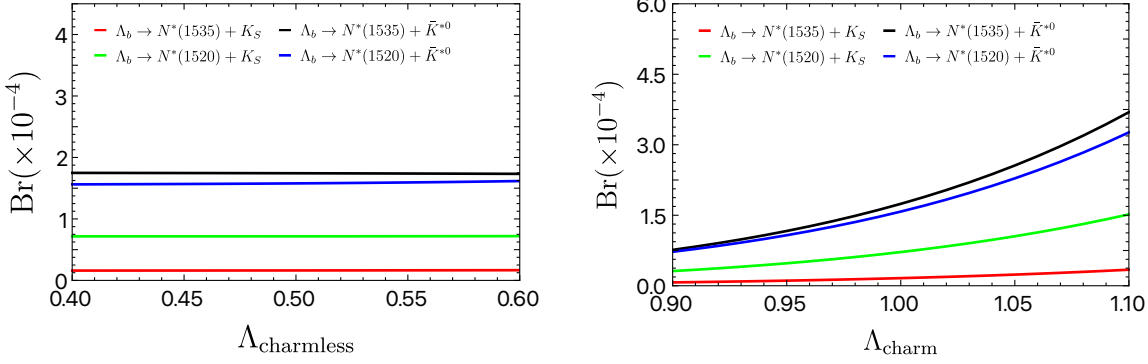


Figure 3: The dependence of the average branching ratios of  $\Lambda_b \rightarrow N^*(1535, 1520)K_S/\bar{K}^{*0}$  on the model parameters  $\Lambda_{\text{charmless}}$  and  $\Lambda_{\text{charm}}$ .

and the direct  $CP$  asymmetry can be expressed in terms of partial wave amplitudes as

$$a_{CP}^{\text{dir}} = \frac{|S|^2 - |\bar{S}|^2 + |P|^2 - |\bar{P}|^2}{|S|^2 + |\bar{S}|^2 + |P|^2 + |\bar{P}|^2} . \quad (18)$$

This formula indicates that the global direct  $CP$  asymmetry can be regarded as a weighted combination of  $a_{CP}^S$  and  $a_{CP}^P$ . Consequently, if there is a cancellation between different partial waves, the total direct  $CP$  asymmetry will be relatively suppressed. In Table. 5, we present the results of the direct  $CP$  asymmetries and partial wave  $CP$  asymmetries with the model parameters  $\Lambda_{\text{charm}} = 1.0 \pm 0.1$  and  $\Lambda_{\text{charmless}} = 0.5 \pm 0.1$ .

Table 5: Direct  $CP$  symmetries and partial-wave  $CP$  asymmetries for  $\Lambda_b \rightarrow N^*P/S$ .

Decay channel	$a_{CP}^{\text{dir}} (\%)$	$a_{CP}^S (\%)$	$a_{CP}^P (\%)$
$N^*(1535)K_S$	$0.23^{+0.29}_{-0.39}$	$1.39^{+0.78}_{-0.97}$	$0.15^{+0.27}_{-0.36}$
$N^*(1535)K_0^*(700)$	$13.2^{+4.50}_{-4.00}$	$17.93^{+1.20}_{-1.10}$	$-14.4^{+19.0}_{-15.4}$
$N^*(1535)f_0(500)$	$-64.6^{+16.6}_{-15.4}$	$-57.6^{+15.5}_{-15.3}$	$-83.3^{+20.7}_{-15.8}$
$N^*(1535)f_0(980)$	$-42.2^{+15.7}_{-21.5}$	$-42.4^{+14.6}_{-20.2}$	$-39.7^{+37.3}_{-46.5}$
$N^*(1520)K_S$	$-1.89^{+1.26}_{-2.12}$	$-1.66^{+1.10}_{-1.83}$	$-4.42^{+3.00}_{-5.49}$
$N^*(1520)K_0^*(700)$	$10.30^{+3.70}_{-3.50}$	$9.80^{+3.60}_{-3.40}$	$60.80^{+19.1}_{-33.5}$
$N^*(1520)f_0(500)$	$-36.6^{+12.8}_{-7.2}$	$-41.4^{+9.2}_{-0.7}$	$-26.1^{+29.2}_{-21.3}$
$N^*(1520)f_0(980)$	$-26.6^{+9.1}_{-11.8}$	$-25.5^{+11.0}_{-14.6}$	$-29.2^{+9.3}_{-12.2}$
$N^*(1535)\bar{K}^{*0}$	$0.77^{+0.28}_{-0.23}$	—	—
$N^*(1535)\rho(770)$	$12.30^{+6.10}_{-4.60}$	—	—
$N^*(1535)\phi$	—	—	—
$N^*(1520)\bar{K}^{*0}$	$2.66^{+3.09}_{-1.87}$	—	—
$N^*(1520)\rho(770)$	$-46.7^{+13.3}_{-13.6}$	—	—
$N^*(1520)\phi$	—	—	—

A basic analysis of the CKM matrix elements and Wilson coefficients of the amplitudes can account for the smallness of  $CP$  violation in certain decay channels. Taking  $\Lambda_b \rightarrow N^* K_S$  for instance, the dominant amplitudes of the tree-level triangle diagrams are proportional to  $V_{cb} V_{cs}^* a_1$ , which is of the order of  $\lambda^2 a_1$ . In contrast, the dominant amplitudes of the penguin-level triangle diagrams are proportional to  $V_{tb} V_{ts}^* a_4$ , which is of the order of  $\lambda^2 a_4$ . Therefore, the direct  $CP$  asymmetry is found to be of the order of  $a_4/a_2 \sim 1\%$ , in agreement with our calculation, and the analogous analysis can be applied to the remaining decay channels.

In Figure 4 and 5, we present the variation of the direct  $CP$  asymmetries for the  $\Lambda_b \rightarrow N^*(1535, 1520) K_S/\bar{K}^{*0}$  and partial wave  $CP$  asymmetries for  $\Lambda_b \rightarrow N^*(1535, 1520) K_S$  with respect to model parameters  $\Lambda_{\text{charmless}}$  and  $\Lambda_{\text{charm}}$ , respectively. Distinct from the charm decays [16] where predictions for  $CP$  asymmetries are basically independent on the model parameter, the results here show visible dependencies on both the model parameters  $\Lambda_{\text{charm}}$  and  $\Lambda_{\text{charmless}}$ . The reason is as follows. The  $CP$  asymmetries are approximately proportional to the ratios of the penguin and tree amplitudes,  $|\mathcal{A}_P/\mathcal{A}_T|$ . In charm decays,  $\mathcal{A}_P$  and  $\mathcal{A}_T$  have similar dependencies on one single parameter  $\Lambda_{\text{charmless}}$ , and thus the dependence get canceled in the  $CP$  violation [16]. However, in the bottom decays,  $\mathcal{A}_P$  basically only depend on  $\Lambda_{\text{charmless}}$ , and the dominant contributions to  $\mathcal{A}_T$  depend on  $\Lambda_{\text{charm}}$ . Therefore, variation of both the parameters change values of  $CP$  asymmetries in bottom decays.

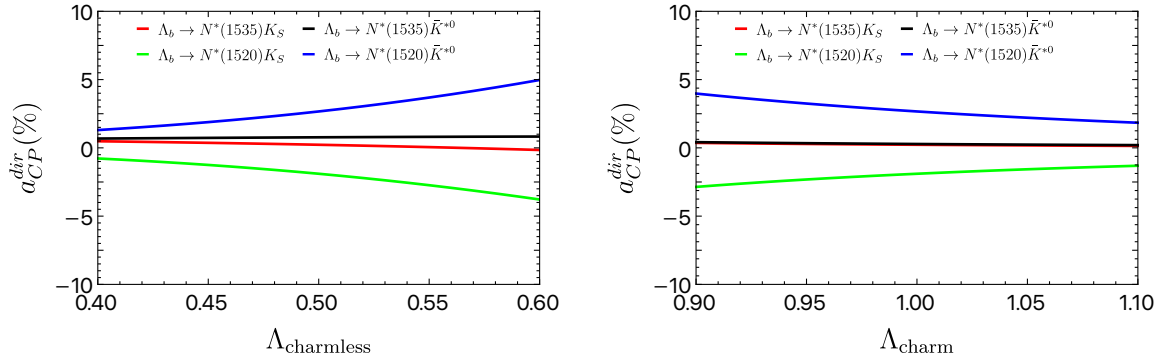


Figure 4: The dependence of the direct  $CP$  asymmetries for  $\Lambda_b \rightarrow N^*(1535, 1520) K_S/\bar{K}^{*0}$  on the model parameters  $\Lambda_{\text{charmless}}$  and  $\Lambda_{\text{charm}}$ .

In the  $\Lambda_b \rightarrow N^* f_0(500, 980)$  processes, the  $f_0(500, 980)$  are scalar mesons with quantum numbers  $I^G(J^P) = 0^+(0^{++})$ . Their internal structure is believed to go well beyond a simple quark-antiquark ( $q\bar{q}$ ) configuration. This conventional interpretation is disfavored by the mass pattern, large- $N_c$  arguments, and various phenomenological studies [45], leading to its common interpretation as either a compact tetraquark or a  $K\bar{K}$  bound state [46]. However, since the possibility of a  $q\bar{q}$  composition has not been completely ruled out, we treat it as a conventional quark-antiquark state in this work. Based on this assumption, our theoretical results provide useful insights into the investigation of its internal structure. It should be noted that the contributions from certain triangle diagrams are temporarily neglected in our calculation, due to the lack of the corresponding coupling constants. Future studies will enable a more precise treatment of these contributions.

For the decay channel  $\Lambda_b \rightarrow N^*(1535) K_0^*(700)$ , the global direct  $CP$  asymmetry  $a_{CP}^{\text{dir}}$  is about 13.2%, whereas  $a_{CP}^S$ ,  $a_{CP}^P$  reaches up to 18.93% and  $-14.4\%$ , respectively, indicating a mild cancellation between the  $S$ - and  $P$ -wave contributions. Such a phenomenon

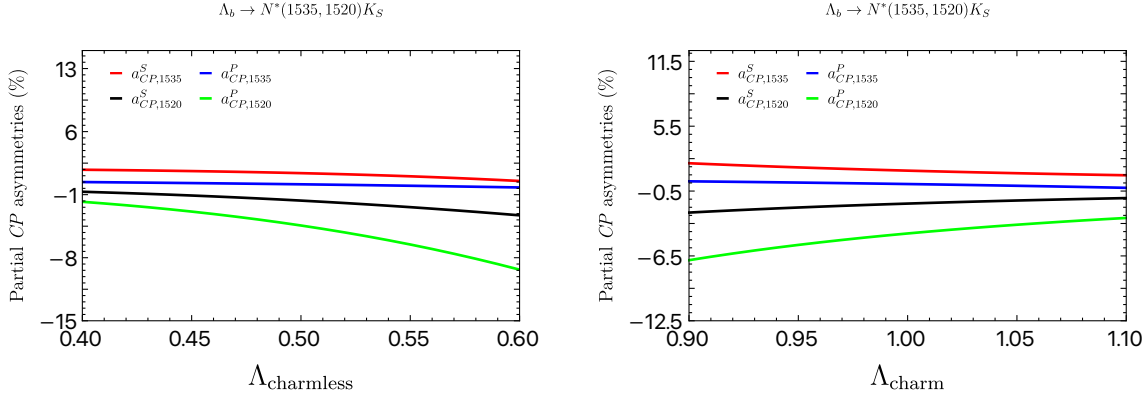


Figure 5: The dependence of the partial wave  $CP$  asymmetries for  $\Lambda_b \rightarrow N^*(1535, 1520)K_S$  on the model parameters  $\Lambda_{\text{charmless}}$  and  $\Lambda_{\text{charm}}$ .

was first observed in Ref. [47], where a perturbative QCD calculation was performed for  $\Lambda_b \rightarrow p\pi^-/K^-$  decays.

For the decay channel  $\Lambda_b \rightarrow N^*(1520)K_0^*(700)$ , although the  $P$ -wave  $CP$  asymmetry  $a_{CP}^P$  reaches up to  $\sim 60\%$ , the global direct  $CP$  asymmetry  $a_{CP}^{\text{dir}}$  is only  $\sim 10\%$ , staying close to the  $S$ -wave  $CP$  asymmetry of this channel. This phenomenon originates from the  $S$ -wave dominance of the branching ratio of this channel. As one can see from Table. 4, the  $S$ -wave branching ratio is larger than the  $P$ -wave one by two orders of magnitude. By varying the model parameters, we find the ratio is  $\frac{Br_S}{Br_P} = 115^{+93}_{-64}$ .

For the decay channel  $\Lambda_b \rightarrow N^*\phi$ , no  $CP$  violation is expected, as only purely penguin amplitudes contribute. Consequently, neither a strong nor a weak phase difference arises.

### 3.4 Asymmetry parameters

For the  $\Lambda_b \rightarrow N^*P/S$  and  $\Lambda_b \rightarrow N^*V$  processes, the asymmetry parameters quantify the differences among the squared magnitudes of distinct helicity amplitudes. These observables serve as sensitive probes of the angular distributions of the final-state particles, thereby providing deeper insight into the helicity structure of the weak Hamiltonian. Moreover, they offer valuable information on the angular correlations and dynamical features of the strong interaction. In the case of the  $\Lambda_b \rightarrow N^*P/S$  processes, the decay asymmetry parameters are defined as [43, 48]

$$\alpha = \frac{|H_{+1/2}|^2 - |H_{-1/2}|^2}{|H_{+1/2}|^2 + |H_{-1/2}|^2}, \quad \beta = \frac{2\text{Im}(H_{+1/2}H_{-1/2}^*)}{|H_{+1/2}|^2 + |H_{-1/2}|^2}, \quad \gamma = \frac{2\text{Re}(H_{+1/2}H_{-1/2}^*)}{|H_{+1/2}|^2 + |H_{-1/2}|^2}, \quad (19)$$

and the averaged asymmetry parameters and their corresponding  $CP$  asymmetries are given by Ref. [49]

$$\begin{aligned} \langle \alpha \rangle &= \frac{\alpha - \bar{\alpha}}{2}, & \langle \beta \rangle &= \frac{\beta - \bar{\beta}}{2}, & \langle \gamma \rangle &= \frac{\gamma + \bar{\gamma}}{2}, \\ a_{CP}^\alpha &= \frac{\alpha + \bar{\alpha}}{2}, & a_{CP}^\beta &= \frac{\beta + \bar{\beta}}{2}, & a_{CP}^\gamma &= \frac{\gamma - \bar{\gamma}}{2}. \end{aligned} \quad (20)$$

One can refer to [50] for alternative definitions. The corresponding results are summarized in Table. 6, and we further display the dependence of the average of the decay asymmetry

parameters  $\langle\alpha\rangle$ ,  $\langle\beta\rangle$ ,  $\langle\gamma\rangle$  for the  $\Lambda_b \rightarrow N^* K_S$  process on the two model parameters in Fig. 6. It shows that the three decay asymmetry parameters exhibit a very weak dependence on the two model parameters, as the model dependence is largely canceled out in this definition.

Table 6: Decay asymmetry parameters and their corresponding  $CP$  asymmetries of  $\Lambda_b \rightarrow N^* P/S$ .

Decay channel	$\langle\alpha\rangle$	$a_{CP}^\alpha(10^{-2})$	$\langle\beta\rangle$	$a_{CP}^\beta(10^{-2})$	$\langle\gamma\rangle$	$a_{CP}^\gamma(10^{-2})$
$N^*(1535)K_S$	$-0.10^{+0.01}_{-0.02}$	$-0.07^{+0.42}_{-0.22}$	$-0.47^{+0.00}_{-0.01}$	$-0.25^{+0.07}_{-0.11}$	$-0.87^{+0.00}_{-0.01}$	$0.14^{+0.07}_{-0.07}$
$N^*(1535)K_0^*(700)$	$-0.62^{+0.06}_{-0.02}$	$19.30^{+7.47}_{-8.04}$	$0.37^{+0.20}_{-0.20}$	$39.93^{+7.53}_{-8.59}$	$0.53^{+0.11}_{-0.16}$	$5.67^{+3.12}_{-2.07}$
$N^*(1535)f_0(500)$	$0.55^{+0.09}_{-0.13}$	$-27.38^{+11.29}_{-15.92}$	$0.52^{+0.06}_{-0.21}$	$10.00^{+3.49}_{-14.81}$	$0.57^{+0.11}_{-0.08}$	$17.53^{+11.92}_{-7.60}$
$N^*(1535)f_0(980)$	$-0.06^{+0.06}_{-0.17}$	$40.0^{+1.98}_{-5.40}$	$0.08^{+0.06}_{-0.06}$	$35.39^{+3.32}_{-2.66}$	$0.84^{+0.00}_{-0.01}$	$-0.49^{+9.23}_{-4.40}$
$N^*(1520)K_S$	$0.43^{+0.02}_{-0.01}$	$0.99^{+0.68}_{-1.13}$	$0.36^{+0.03}_{-0.05}$	$0.19^{+0.28}_{-0.17}$	$0.83^{+0.01}_{-0.01}$	$0.44^{+0.52}_{-0.29}$
$N^*(1520)K_0^*(700)$	$0.14^{+0.09}_{-0.13}$	$4.45^{+3.55}_{-2.09}$	$-0.11^{+0.05}_{-0.06}$	$-2.45^{+2.03}_{-3.60}$	$0.98^{+0.01}_{-0.02}$	$-0.88^{+0.34}_{-0.24}$
$N^*(1520)f_0(500)$	$-0.10^{+0.17}_{-0.14}$	$36.47^{+0.00}_{-10.37}$	$-0.85^{+0.04}_{-0.04}$	$-7.15^{+6.45}_{-2.98}$	$0.34^{+0.11}_{-0.10}$	$-7.61^{+10.74}_{-9.60}$
$N^*(1520)f_0(980)$	$-0.49^{+0.08}_{-0.04}$	$10.27^{+4.41}_{-2.95}$	$-0.77^{+0.04}_{-0.05}$	$-5.61^{+2.45}_{-3.15}$	$0.39^{+0.03}_{-0.02}$	$1.69^{+4.93}_{-7.54}$

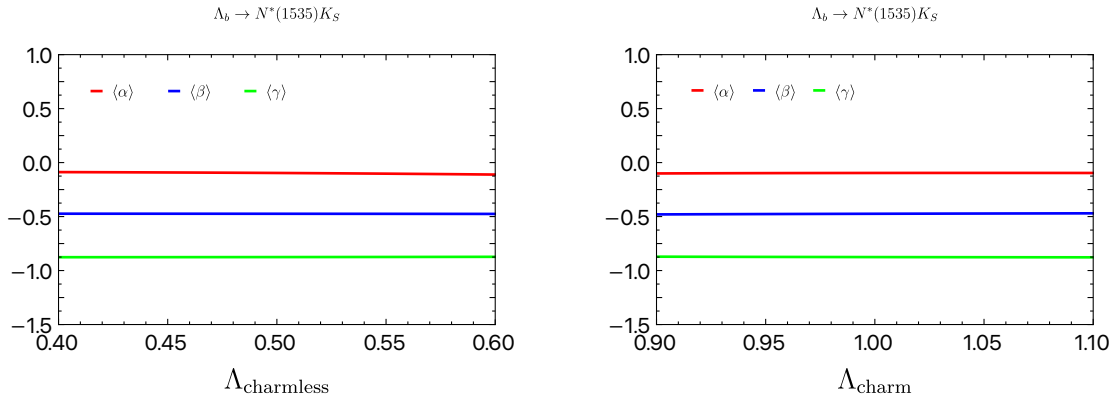


Figure 6: The dependence of the decay asymmetry parameters for  $\Lambda_b \rightarrow N^* K_S$  on the model parameters  $\Lambda_{\text{charmless}}$  and  $\Lambda_{\text{charm}}$ .

In the case of the  $\Lambda_b \rightarrow N^*(1535)V$  processes, the decay asymmetry parameters are defined as [43, 48]

$$\begin{aligned} \alpha' &= \frac{|H_{+1,+1/2}|^2 - |H_{-1,-1/2}|^2}{|H_{+1,+1/2}|^2 + |H_{-1,-1/2}|^2}, & \beta' &= \frac{|H_{0,+1/2}|^2 - |H_{0,-1/2}|^2}{|H_{0,+1/2}|^2 + |H_{0,-1/2}|^2}, \\ \gamma' &= \frac{|H_{+1,+1/2}|^2 + |H_{-1,-1/2}|^2}{|H_{0,+1/2}|^2 + |H_{0,-1/2}|^2}, \end{aligned} \quad (21)$$

and the longitudinal polarization of  $N^*$  is characterized by

$$P_L = \frac{|H_{+1,+1/2}|^2 - |H_{-1,-1/2}|^2 + |H_{0,+1/2}|^2 - |H_{0,-1/2}|^2}{|H_{+1,+1/2}|^2 + |H_{-1,-1/2}|^2 + |H_{0,+1/2}|^2 + |H_{0,-1/2}|^2}, \quad (22)$$

these parameters are not independent and their relation is shown as follows

$$P_L = \frac{\beta' + \alpha' \cdot \gamma'}{1 + \gamma'} . \quad (23)$$

The observable  $\alpha'$  was first proposed by T. D. Lee and C. N. Yang in Ref. [20], which can be extracted from the angular distributions of the  $N^*(1535)$  in the rest frame of  $\Lambda_b$ ,

$$\frac{d\Gamma}{dcos\theta} \propto 1 + \mathcal{P}\alpha'cos\theta , \quad (24)$$

where  $\mathcal{P}$  is the polarization of  $\Lambda_b^0$  [51], and  $\theta$  is the angle between the direction of the polarization of  $\Lambda_b^0$  and the momentum of  $N^*(1535)$ . The other two parameters  $\beta', \gamma'$  could be determined by measuring the polarization of  $N^*(1535)$  in the final state [52, 53]. The decay asymmetry parameters for the channel  $\Lambda_b \rightarrow N^*(1535)V$ , calculated with model parameters  $\Lambda_{\text{charm}} = 1.0 \pm 0.1$  and  $\Lambda_{\text{charmless}} = 0.5 \pm 0.1$ , are presented in Table. 7. Then we illustrate the dependence of the four decay asymmetry parameters for the process  $\Lambda_b \rightarrow N^*(1535)\bar{K}^{*0}$  on the model parameters  $\Lambda_{\text{charm}}$  and  $\Lambda_{\text{charmless}}$  in Fig. 7, and find that they are rather insensitive to the variations of the two model parameters.

Table 7: Decay asymmetry parameters and their corresponding  $CP$  asymmetries for  $\Lambda_b \rightarrow N^*(1535)V$  processes.

Decay channel	$\langle \alpha' \rangle$	$a_{CP}^{\alpha'}(10^{-2})$	$\langle \beta' \rangle$	$a_{CP}^{\beta'}(10^{-2})$
$N^*(1535)\bar{K}^{*0}$	$0.75^{+0.01}_{-0.01}$	$0.28^{+0.20}_{-0.24}$	$-0.794^{+0.01}_{-0.01}$	$0.36^{+0.27}_{-0.18}$
$N^*(1535)\rho(770)$	$0.60^{+0.07}_{-0.10}$	$18.74^{+9.28}_{-8.71}$	$-0.713^{+0.076}_{-0.083}$	$1.35^{+2.06}_{-2.77}$
Decay channel	$\langle \gamma' \rangle$	$a_{CP}^{\gamma'}(10^{-2})$	$\langle P_L \rangle$	$a_{CP}^{P_L}$
$N^*(1535)\bar{K}^{*0}$	$1.76^{+0.05}_{-0.03}$	$-0.13^{+0.03}_{-0.07}$	$-0.23^{+0.01}_{-0.06}$	$0.43^{+0.01}_{-0.01}$
$N^*(1535)\rho(770)$	$0.96^{+0.37}_{-0.17}$	$64.00^{+28.53}_{-19.46}$	$0.35^{+0.09}_{-0.08}$	$-0.13^{+0.04}_{-0.09}$

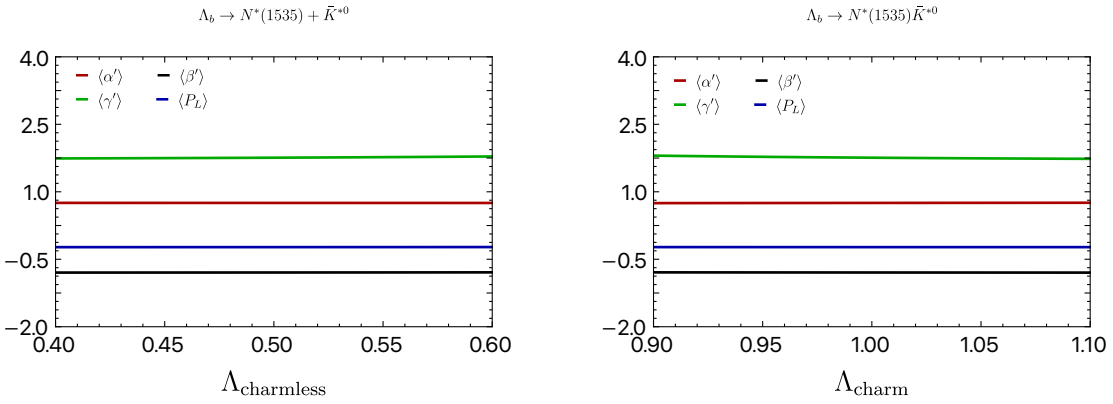


Figure 7: The dependence of the average of decay asymmetry parameters for  $\Lambda_b \rightarrow N^*(1535)\bar{K}^{*0}$  on the model parameters  $\Lambda_{\text{charmless}}$  and  $\Lambda_{\text{charm}}$ .

In the case of the  $\Lambda_b \rightarrow N^*(1520)V$  processes, the decay width is defined as

$$\begin{aligned} \Gamma(\Lambda_b \rightarrow N^*(1520)V) = & \frac{p_c}{8\pi m_{\Lambda_b}^2} \frac{1}{2} (|H_{+1,+3/2}|^2 + |H_{0,+1/2}|^2 + |H_{-1,-1/2}|^2 + |H_{+1,+1/2}|^2 \\ & + |H_{0,-1/2}|^2 + |H_{-1,-3/2}|^2) , \end{aligned} \quad (25)$$

and the two asymmetry parameters  $A_T \sin(2\varphi_R)$  and  $A_T \sin(\varphi_R)$  are introduced in Ref. [54, 55]

$$\begin{aligned} A_T(\sin 2\varphi_R) &= Im(H_{+3/2,+1}H_{-1/2,-1}^*) - Im(H_{+1/2,+1}H_{-3/2,-1}^*) , \\ A_T(\sin \varphi_R) &= Im(H_{+3/2,+1}H_{+1/2,0}^*) - Im(H_{-1/2,0}H_{-3/2,-1}) . \end{aligned} \quad (26)$$

As they correspond to the  $T$ -odd and Parity-odd quantities, we define

$$\begin{aligned} a_{CP}(\sin \varphi_R) &= \frac{A_T(\sin \varphi_R) + \bar{A}_T(\sin \varphi_R)}{\sum_{\lambda_f, \lambda_M} |H_{\lambda_f, \lambda_M}|^2 + |\bar{H}_{\lambda_f, \lambda_M}|^2}, \\ a_{CP}(\sin 2\varphi_R) &= \frac{A_T(\sin 2\varphi_R) + \bar{A}_T(\sin 2\varphi_R)}{\sum_{\lambda_f, \lambda_M} |H_{\lambda_f, \lambda_M}|^2 + |\bar{H}_{\lambda_f, \lambda_M}|^2}. \end{aligned} \quad (27)$$

Since the helicity amplitudes can be expressed as linear combinations of partial waves, the asymmetry parameters  $A_T(\sin \varphi_R)$  and  $A_T(\sin 2\varphi_R)$  reduce to the imaginary part of the interference terms between partial waves with opposite parities. In addition to the  $T$ -odd observables  $\sin \varphi_R$  and  $\sin(2\varphi_R)$ , the quantities  $\cos \varphi_R$  and  $\cos(2\varphi_R)$  are also valuable for constructing  $T$ -even  $CP$ -violating observables. Similar to  $A_T \sin(\varphi_R)$  and  $A_T \sin(2\varphi_R)$ , we can define

$$\begin{aligned} A_T(\cos 2\varphi_R) &= \text{Re}(H_{+3/2,+1}H_{-1/2,-1}^*) + \text{Re}(H_{+1/2,+1}H_{-3/2,-1}^*), \\ A_T(\cos \varphi_R) &= \text{Re}(H_{+3/2,+1}H_{+1/2,0}^*) + \text{Re}(H_{-1/2,0}H_{-3/2,-1}^*), \end{aligned} \quad (28)$$

and the other two  $CP$ -violating observables can be written as

$$\begin{aligned} a_{CP}(\cos \varphi_R) &= \frac{A_T(\cos \varphi_R) - \bar{A}_T(\cos \varphi_R)}{\sum_{\lambda_f, \lambda_M} |H_{\lambda_f, \lambda_M}|^2 + |\bar{H}_{\lambda_f, \lambda_M}|^2}, \\ a_{CP}(\cos 2\varphi_R) &= \frac{A_T(\cos 2\varphi_R) - \bar{A}_T(\cos 2\varphi_R)}{\sum_{\lambda_f, \lambda_M} |H_{\lambda_f, \lambda_M}|^2 + |\bar{H}_{\lambda_f, \lambda_M}|^2}, \end{aligned} \quad (29)$$

the two  $CP$  asymmetries  $a_{CP}(\cos \varphi_R)$  and  $a_{CP}(\cos 2\varphi_R)$  are complementary to  $a_{CP}(\sin \varphi_R)$  and  $a_{CP}(\sin 2\varphi_R)$  [55]. The corresponding results are listed in Table. 8.

Table 8:  $CP$  asymmetries of decay parameters in  $\Lambda_b \rightarrow N^*(1520)V$  decays.

Decay channel	$a_{cp}(\sin \varphi_R)(\%)$	$a_{cp}(\sin 2\varphi_R)(\%)$	$a_{cp}(\cos \varphi_R)(\%)$	$a_{cp}(\cos 2\varphi_R)(\%)$
$N^*(1520)\bar{K}^{*0}$	$0.34^{+0.05}_{-0.08}$	$-1.17^{+0.16}_{-0.24}$	$0.17^{+0.05}_{-0.12}$	$0.09^{+0.06}_{-0.03}$
$N^*(1520)\rho(770)$	$-4.79^{+0.67}_{-0.50}$	$0.11^{+0.34}_{-0.19}$	$0.51^{+0.67}_{-0.10}$	$-0.95^{+0.24}_{-1.40}$

## 4 Conclusion

In this work, we investigate the charmless non-leptonic two-body decays of  $\Lambda_b \rightarrow N^* M$  with  $M = K_S, K_0^*(700), f_0(500, 980), \rho(770), \bar{K}^{*0}, \phi$ , within the framework of the final-state rescattering mechanism. These decay channels are of particular interest due to their relevance for understanding non-perturbative QCD dynamics at the bottom-quark mass scale and their potential for observing  $CP$  violation. In contrast to previous studies based on the optical theorem, which focused on the imaginary parts of decay amplitudes, our approach performs a complete calculation of the long-distance contributions from triangle

diagrams. The improved treatment naturally generates the strong phases essential for  $CP$  violation, thereby allowing for more precise predictions of the observables in  $\Lambda_b$  decays.

Based on the available experimental data for the branching fractions and  $CP$  asymmetries of  $\Lambda_b \rightarrow pK^-$  and  $\Lambda_b \rightarrow p\pi^-$ , we introduce two model parameters,  $\Lambda_{\text{charm}}$  and  $\Lambda_{\text{charmless}}$ . These parameters provide robust theoretical inputs for subsequent phenomenological analysis and offer a deeper insight into the underlying dynamics of  $\Lambda_b$  decays. We further study a series of  $\Lambda_b \rightarrow N^*(1535, 1520)M$  decay channels with  $M = K_S, K_0^*(700), f_0(500, 980), \rho(770), \bar{K}^{*0}, \phi$ , and provide predictions for various physical observables, including branching ratios, direct  $CP$  asymmetries, partial-wave amplitude  $CP$  asymmetries, and decay asymmetry parameters. We also find a significant cancellation between the different partial wave  $CP$  violations of the decay channel  $\Lambda_b \rightarrow N^*(1520)K_0^*$ , as discussed in Ref. [47]. Moreover, we estimate several strong coupling constants with  $SU(4)$  flavor symmetry that are not yet experimentally accessible.

Future improvements in theoretical precision will require (i) more accurate determinations of form factors, (ii) reduced uncertainties in strong coupling constants, and (iii) the construction of experimentally measurable observables with minimal model dependence. The theoretical framework employed in this work provides a systematic approach for investigating various charmless non-leptonic two-body  $\Lambda_b$  decays involving excited nucleons in the final state. Our results, as primary decay processes, are expected to contribute to the  $CP$  asymmetries in subsequent four-body decay channels, such as  $\Lambda_b^0 \rightarrow p\pi^-\pi^+\pi^-$ , which are anticipated to be measured by the LHCb experiment. Further applications to numerous  $\Lambda_b$  decay modes are expected in future work.

**Acknowledgement** The authors are very grateful to Jian-Peng Wang, Cai-Ping Jia, Zhu-Ding Duan for helpful discussions. This work is supported by the National Science Foundation of China under Grant No. 12335003, No. 12522506 and No. 12375086, and by the Fundamental Research Funds for the Central Universities under No. lzujbky-2023-stlt01 and lzujbky-2024-oy02.

## A Effective Lagrangian

- The effective Lagrangian for pseudoscalar meson octet  $P_8$ , vector meson  $V$ , charmed baryon sextets  $B_6$  and anti-triplets  $B_{\bar{3}}$ :

$$\begin{aligned}
\mathcal{L}_{VPP} &= \frac{ig_{VPP}}{\sqrt{2}} Tr[V^\mu [P, \partial_\mu P]] , \\
\mathcal{L}_{VVV} &= \frac{ig_{VVV}}{\sqrt{2}} Tr[(\partial_\nu V_\mu V^\mu - V^\mu \partial_\nu V_\mu) V^\nu] , \\
\mathcal{L}_{PB_6 B_6} &= g_{PB_6 B_6} Tr[\bar{B}_6 i \gamma_5 P B_6] , \\
\mathcal{L}_{VB_6 B_6} &= f_{1VB_6 B_6} Tr[\bar{B}_6 \gamma_\mu V^\mu B] + \frac{f_{2VB_6 B_6}}{m_6 + m_6} Tr[\bar{B}_6 \sigma_{\mu\nu} \partial^\mu V^\nu B] , \\
\mathcal{L}_{PB_6 B_{\bar{3}}} &= g_{PB_6 B_{\bar{3}}} Tr[\bar{B}_6 i \gamma_5 P B_{\bar{3}}] + h.c. , \\
\mathcal{L}_{VB_6 B_{\bar{3}}} &= f_{1VB_6 B_{\bar{3}}} Tr[\bar{B}_6 \gamma_\mu V^\mu B_{\bar{3}}] + \frac{f_{2VB_6 B_{\bar{3}}}}{m_3 + m_6} Tr[\bar{B}_6 \sigma_{\mu\nu} \partial^\mu V^\nu B_{\bar{3}}] + h.c. .
\end{aligned} \tag{30}$$

- The effective Lagrangians involving  $D/D^*$  mesons:

$$\begin{aligned}
\mathcal{L}_{D^* DP} &= -ig_{D^* DP} (D^i \partial^\mu P_{ij} D_\mu^{*j+} - D_\mu^{*i} \partial^\mu P_{ij} D^{j+}) , \\
\mathcal{L}_{D^* D^* P} &= \frac{1}{2} g_{D^* D^* P} \epsilon_{\mu\nu\alpha\beta} D_i^{*\mu} \partial^\nu P^{ij} \overleftrightarrow{\partial}^\alpha D_j^{*\beta+} , \\
\mathcal{L}_{DDV} &= -ig_{DDV} D_i \overleftrightarrow{\partial}_\mu D^{j+} (V^\mu)_j^i , \\
\mathcal{L}_{D^* DV} &= -2f_{D^* DV} \epsilon_{\mu\nu\alpha\beta} (\partial^\mu V^\nu)_j^i (D_i \overleftrightarrow{\partial}^\alpha D^{*\beta j+} - D_i^{*\beta} \overleftrightarrow{\partial}^\alpha D^{j+}) , \\
\mathcal{L}_{D^* D^* V} &= ig_{D^* D^* V} D_i^{*\nu+} \overleftrightarrow{\partial}_\mu D_\nu^{*j} (V^\mu)_j^i + 4if_{D^* D^* V} D_{i\mu}^{*+} (\partial^\mu V^\nu - \partial^\nu \partial^\mu)_j^i D_\nu^{*j} .
\end{aligned} \tag{31}$$

- The effective Lagrangians involving  $N^*(1535, 1520)$ :

$$\begin{aligned}
\mathcal{L}_{\pi N N^*}^{1520} &= \frac{f_{\pi N N^*}^{1520}}{m_\pi} \bar{\psi} \chi^\dagger \gamma_5 \partial_\mu \vec{\phi} \cdot \vec{\tau} \chi \psi_\mu + h.c. , \\
\mathcal{L}_{\pi N N^*}^{1535} &= \frac{if_{\pi N N^*}^{1535}}{m_\pi} \bar{\psi} \chi^\dagger \gamma_\mu \partial_\mu \vec{\phi} \cdot \vec{\tau} \chi \psi_{N^*} + h.c. , \\
\mathcal{L}_{\omega N N^*}^{1520} &= \frac{ig_{\omega N N^*}^{1520}}{m_\omega^2} \bar{\psi}_N \sigma_{\mu\nu} \partial_\nu \partial_\kappa \omega_\mu \psi_\kappa + h.c. , \\
\mathcal{L}_{\omega N N^*}^{1535} &= -\frac{ig_{\omega N N^*}^{1535}}{m_\omega^2} \bar{\psi}_N \gamma_5 [\gamma_\mu \partial^2 - (m^* + m_N) \partial_\mu] \omega_\mu \psi_{N^*} + h.c. , \\
\mathcal{L}_{\rho N N^*}^{1520} &= \frac{ig_{\rho N N^*}^{1520}}{m_\rho^2} \bar{\psi} \chi^\dagger \sigma_{\mu\nu} \partial_\nu \partial_\kappa \vec{\tau} \cdot \vec{\rho}_\mu \chi \psi_\kappa + h.c. , \\
\mathcal{L}_{\rho N N^*}^{1535} &= -\frac{ig_{\rho N N^*}^{1535}}{m_\rho^2} \bar{\psi} \chi^\dagger \gamma_5 [\gamma_\mu \partial^2 - (m^* + m_N) \partial_\mu] \vec{\tau} \cdot \vec{\rho}_\mu \chi \psi_{N^*} + h.c. .
\end{aligned} \tag{32}$$

## B Feynman rules for strong interaction vertices

The corresponding Feynman rules for strong interaction vertices used in this work are as follows:

$$\begin{aligned}
\langle P(p_3)D(k)|i\mathcal{L}_{D^*DP}|D^*(p_1)\rangle &= i^3 g_{D^*DP} \epsilon_\mu(p_1) p_3^\mu , \\
\langle P(p_3)D^*(k)|i\mathcal{L}_{D^*D^*P}|D^*(p_1)\rangle &= i^3 \frac{1}{2} g_{D^*D^*P} \epsilon_{\mu\nu\alpha\beta} \epsilon^\mu(p_1) [p_3^\nu p_3^\alpha \epsilon^{*\beta}(k) - p_3^\nu k^\alpha \epsilon^{*\beta}(k)] , \\
\langle P(p_3)|i\mathcal{L}_{VPP}|P(k)V(p_1)\rangle &= i^3 \frac{g_{VPP}}{\sqrt{2}} \epsilon^{*\mu}(p_1) (p_3 + k)_\mu , \\
\langle P(p_3)|i\mathcal{L}_{VVP}|V(p_1)V(k)\rangle &= i^3 \frac{4g_{VVP}}{f_P} \epsilon^{\mu\nu\alpha\beta} p_{1\mu} \epsilon_\nu(p_1) k_\alpha \epsilon_\beta(k) , \\
\langle K_0^*(700)(p_3)D(k)|i\mathcal{L}_{K_0^*(700)DD}|D_s(p_1)\rangle &= -i^3 \gamma_{\kappa K\pi} p_{1\mu} k^\mu , \\
\langle \sigma(p_3)|i\mathcal{L}_{\sigma DD}|D(p_1)D(k)\rangle &= -i^3 \frac{\gamma_{\sigma DD}}{\sqrt{2}} p_1 \cdot k , \\
\langle \sigma(p_3)\Lambda_c(k)|i\mathcal{L}_{\sigma NN}|\Lambda_c(p_2)\rangle &= i g_{\sigma NN} \bar{u}(k, s_k) u(p_2, s_2) , \\
\langle f_0(980)(p_3)|i\mathcal{L}_{f_0 DD}|D(p_1)D(k)\rangle &= i \frac{1}{2} g_{f_0 \pi\pi} = i \frac{1}{2} g_{f_0 DD} , \\
\langle N^*(1520)(p_4)|i\mathcal{L}_{\Lambda_c DN^*}|\Lambda_c(p_2)D(k)\rangle &= -i^2 \frac{f_{\pi NN^*}^{1520}}{m_\pi} \bar{u}_\mu(p_4, s_4) \gamma_5 k^\mu u(p_2, s_2) , \\
\langle N^*(1535)(p_4)|i\mathcal{L}_{\Lambda_c DN^*}|\Lambda_c(p_2)D(k)\rangle &= -i^3 \frac{f_{\pi NN^*}^{1535}}{m_\pi} \bar{u}(p_4, s_4) \gamma_\mu k^\mu u(p_2, s_2) , \\
\langle N^*(1520, p_4)|i\mathcal{L}_{VNN^*}^{1520}|\Lambda_c(p_2)D^*(k)\rangle &= i^4 \frac{g_{\rho NN^*}^{1520}}{m_\rho^2} \bar{u}_\alpha(p_4, s_4) \sigma_{\mu\nu} k^\nu k^\alpha \epsilon^{*\mu}(k) u(p_2, s_2) , \\
\langle N^*(1535)(p_4)|i\mathcal{L}_{\rho NN^*}^{1535}|\Lambda_c(p_2)D^*(k)\rangle &= -i^2 \frac{g_{\rho NN^*}^{1535}}{m_\rho^2} \bar{u}(p_4, s_4) [\gamma_\mu(-k^2) - (m_2 + m_4) \\
&\quad \times (-ik_\mu)] \times \gamma_5 \epsilon^\mu(k) u(p_2, s_2) , \\
\langle N^*(1520)(p_4)V(k)|i\mathcal{L}_{VNN^*}^{1520}|B_8(p_2)\rangle &= -i^4 \frac{g_{\rho NN^*}^{1520}}{m_\rho^2} \bar{u}_\kappa(p_4, s_4) \sigma_{\mu\nu} k^\nu k^\kappa \epsilon^{*\mu}(k) u(p_2, s_2) , \\
\langle N^*(1535)(p_4)V(k)|i\mathcal{L}_{VNN^*}^{1535}|B_8(p_2)\rangle &= i^2 \frac{g_{\rho NN^*}^{1535}}{m_\rho^2} \bar{u}(p_4, s_4) [\gamma_\mu(-k^2) - i(m_2 + m_4) k_\mu] \\
&\quad \times \gamma_5 \epsilon^{*\mu}(k) u(p_2, s_2) , \\
\langle V(p_3)D(k)|i\mathcal{L}_{DDV}|D_s(p_1)\rangle &= -i^3 g_{DDV} (k_\mu + p_{1\mu}) \epsilon^{*\mu}(p_3) , \\
\langle V(p_3)D(k)|i\mathcal{L}_{D^*DV}|D_s^{*-}(p_1)\rangle &= -2i^3 f_{D^*DV} \epsilon_{\mu\nu\alpha\beta}(p_1) p_3^\mu (k + p_1)^\alpha \epsilon^{*\nu}(p_3) \epsilon^\beta(p_1) , \\
\langle V(p_3)D^*(k)|i\mathcal{L}_{D^*D^*V}|D_s^*(p_1)\rangle &= i^3 g_{D^*D^*V} (k + p_1)_\mu \epsilon^{*\nu}(k) \epsilon_\nu(p_1) \epsilon^{*\mu}(p_3) \\
&\quad + 4i^3 f_{D^*D^*V} \epsilon_\mu^*(k) [p_3^\mu \epsilon^{*\nu}(p_3) - p_3^\nu \epsilon^{*\mu}(p_3)] \epsilon_\nu(p_1) , \\
\langle V(p_3)|i\mathcal{L}_{VVV}|V(p_1)V(k)\rangle &= i^3 \frac{g_{VVV}}{\sqrt{2}} [-k_\nu \epsilon_\mu(k) \epsilon^{*\mu}(p_3) \epsilon^\nu(p_1) - \epsilon_\mu(k) p_{3\nu} \epsilon^{*\mu}(p_3) \\
&\quad \times \epsilon^\nu(p_1) + p_{3\nu} \epsilon_\mu^*(p_3) \epsilon^\mu(p_1) \epsilon^\nu(k) + \epsilon^{*\mu}(p_3) p_{1\nu} \\
&\quad \times \epsilon_\mu(p_1) \epsilon^\nu(k)] , \\
\langle N^*(1535)(p_4)|i\mathcal{L}_{\pi NN^*}^{1535}|\Lambda_c(p_2)D(k)\rangle &= i^3 \frac{f_{\pi NN^*}^{1535}}{m_\pi} \bar{u}(p_4, s_4) \gamma_\mu k^\mu u(p_2, s_2) , \\
\langle N^*(1520)(p_4)|i\mathcal{L}_{\pi NN^*}^{1520}|\Lambda_c(p_2)D(k)\rangle &= i^2 \frac{f_{\pi NN^*}^{1520}}{m_\pi} \epsilon_\mu^*(p_4) \bar{u}(p_4, s_4) \gamma_5 k^\mu u(p_2, s_2) ,
\end{aligned} \tag{33}$$

$$\begin{aligned}
\langle N^*(1535)(p_4) | i\mathcal{L}_{\rho NN^*}^{1535} | \Lambda_c(p_2) D^*(k) \rangle &= -i \frac{g_{\rho NN^*}^{1535}}{m_\rho^2} \bar{u}(p_4, s_4) [\gamma_\mu k^2 - i(m_2 + m_4) k_\mu] \\
&\quad \times \gamma_5 \epsilon^\mu(k) u(p_2, s_2), \\
\langle N^*(1520)(p_4) | i\mathcal{L}_{\rho NN^*}^{1520} | \Lambda_c(p_2) D^*(k) \rangle &= i^3 \frac{g_{\rho NN^*}^{1520}}{m_\rho^2} \epsilon_\kappa^*(p_4) \bar{u}(p_4, s_4) \sigma_{\mu\nu} k^\nu k^\kappa \epsilon^\mu(k) \\
&\quad \times u(p_2, s_2), \\
\langle N^*(1520)(p_4) | i\mathcal{L}_{VNN^*}^{1520} | \Lambda_c(p_2) D^*(k) \rangle &= i^4 \frac{g_{\rho NN^*}^{1520}}{m_\rho^2} \bar{u}_\alpha(p_4, s_4) \sigma_{\mu\nu} k^\nu k^\alpha \epsilon^{*\mu}(k) u(p_2, s_2), \\
\langle N^*(1535)(p_4) | i\mathcal{L}_{\rho NN^*}^{1535} | \Lambda_c(p_2) D^*(k) \rangle &= -i^2 \frac{g_{\rho NN^*}^{1535}}{m_\rho^2} \bar{u}(p_4, s_4) [\gamma_\mu(-k^2) - (m_2 + m_4) \\
&\quad \times (-ik_\mu)] \gamma_5 \epsilon^\mu(k) u(p_2, s_2), \\
\langle N^*(1520)(p_4) V(k) | i\mathcal{L}_{VNN^*}^{1520} | B_8(p_2) \rangle &= -i^4 \frac{g_{\rho NN^*}^{1520}}{m_\rho^2} \bar{u}_\kappa(p_4, s_4) \sigma_{\mu\nu} k^\nu k^\kappa \epsilon^{*\mu}(k) u(p_2, s_2), \\
\langle N^*(1535)(p_4) V(k) | i\mathcal{L}_{VNN^*}^{1535} | B_8(p_2) \rangle &= i^2 \frac{g_{\rho NN^*}^{1535}}{m_\rho^2} \bar{u}(p_4, s_4) [\gamma_\mu(-k^2) - i(m_2 + m_4) k_\mu] \\
&\quad \times \gamma_5 \epsilon^{*\mu}(k) u(p_2, s_2).
\end{aligned} \tag{34}$$

## C Amplitudes of triangle diagrams

The amplitudes of triangle diagrams for the decay  $\Lambda_b \rightarrow N^*(1535, 1520)P_8$  are

$$\begin{aligned}
\mathcal{M}[D^*, B_{\bar{3}}; D]_{1520} &= -i^5 \int \frac{d^4 p}{2\pi^4} g_{D^* D P} \frac{f_{DB_3 N^*}^{1520}}{m_D} \bar{u}_\mu(p_4, s_4) \gamma_5 k^\mu (\not{p}_2 + m_2) [A_1 \gamma_\alpha \gamma_5 \\
&\quad + A_2 \frac{p_{2\alpha}}{m_i} \gamma_5 + B_1 \gamma_\alpha + B_2 \frac{p_{2\alpha}}{m_i}] u(p_i, s_i) (-g^{\alpha\beta} + \frac{p_1^\alpha p_1^\beta}{m_1^2}) p_3^\beta \times \mathcal{F} \times \mathcal{P}, \\
\mathcal{M}[D^*, B_{\bar{3}}; D]_{1535} &= -i^6 \int \frac{d^4 p}{2\pi^4} g_{D^* D P} \frac{f_{DB_3 N^*}^{1535}}{m_D} \bar{u}(p_4, s_4) \gamma_\mu k^\mu (\not{p}_2 + m_2) [A_1 \gamma_\alpha \gamma_5 \\
&\quad + A_2 \frac{p_{2\alpha}}{m_i} \gamma_5 + B_1 \gamma_\alpha + B_2 \frac{p_{2\alpha}}{m_i}] u(p_i, s_i) (-g^{\alpha\beta} + \frac{p_1^\alpha p_1^\beta}{m_1^2}) p_3^\beta \times \mathcal{F} \times \mathcal{P}, \\
\mathcal{M}[D, B_{\bar{3}}; D^*]_{1520} &= -i^8 \int \frac{d^4 p}{(2\pi)^4} g_{D^* D P} \frac{g_{D^* B_{\bar{3}} N^*}^{1520}}{m_{D^*}^2} \bar{u}_\alpha(p_4, s_4) \sigma_{\mu\nu} k^\nu k^\alpha \epsilon^{*\mu}(k) (\not{p}_2 \\
&\quad + m_2) \times [A + B \gamma_5] u(p_i, s_i) \epsilon_\delta^*(k) p_3^\delta \times \mathcal{F} \times \mathcal{P}, \\
\mathcal{M}[D, B_{\bar{3}}; D^*]_{1535} &= -i^6 \int \frac{d^4 p}{(2\pi)^4} g_{D^* D P} \frac{g_{D^* B_{\bar{3}} N^*}^{1535}}{m_{D^*}^2} \bar{u}(p_4, s_4) [\gamma_\mu(-k^2) - (m_2 + m_4) \\
&\quad \times (-ik_\mu)] \times \gamma_5 \epsilon^\mu(k) \times (\not{p}_2 + m_2) [A + B \gamma_5] \times u(p_i, s_i) \epsilon^{*\alpha}(k) p_{3\alpha} \\
&\quad \times \mathcal{F} \times \mathcal{P}, \\
\mathcal{M}[D^*, B_{\bar{3}}; D^*]_{1520} &= i^7 \int \frac{d^4 p}{(2\pi)^4} \frac{1}{2} g_{D^* D^* P} \frac{g_{D^* B_{\bar{3}} N^*}^{1520}}{m_{D^*}^2} \bar{u}_\alpha(p_4, s_4) \sigma_{\mu\nu} k^\nu k^\alpha \epsilon^{*\mu}(k) (\not{p}_2 \\
&\quad + m_2) \times \epsilon^{*\beta}(p_1) \times [A_1 \gamma_\beta \gamma_5 + A_2 \frac{p_{2\beta}}{m_i} \gamma_5 + B_1 \gamma_\beta + B_2 \frac{p_{2\beta}}{m_i}] u(p_i, s_i) \\
&\quad \times \epsilon_{\mu_1 \nu_1 \alpha_1 \beta_1} \times \epsilon^{\mu_1}(p_1) [p_3^{\nu_1} p_3^{\alpha_1} \epsilon^{*\beta_1}(k) - p_3^{\nu_1} k^{\alpha_1} \epsilon^{*\beta_1}(k)] \times \mathcal{F} \times \mathcal{P}, \\
\mathcal{M}[D^*, B_{\bar{3}}; D^*]_{1535} &= -i^5 \int \frac{d^4 p}{(2\pi)^4} \frac{1}{2} g_{D^* D^* P} \frac{g_{D^* B_{\bar{3}} N^*}^{1535}}{m_{D^*}^2} \bar{u}(p_4, s_4) [\gamma_\mu(-k^2) - (m_2 \\
&\quad + m_4) \times (-ik_\mu)] \gamma_5 \epsilon^\mu(k) \times (\not{p}_2 + m_2) \epsilon^{*\nu}(p_1) \times [A_1 \gamma_\nu \gamma_5 + A_2 \frac{p_{2\nu}}{m_i} \\
&\quad \times \gamma_5 + B_1 \gamma_\nu + B_2 \frac{p_{2\nu}}{m_i}] u(p_i, s_i) \times \epsilon_{\mu_1 \nu_1 \alpha_1 \beta_1} \epsilon^{\mu_1}(p_1) [p_3^{\nu_1} p_3^{\alpha_1} \epsilon^{*\beta_1}(k) \\
&\quad - p_3^{\nu_1} k^{\alpha_1} \epsilon^{*\beta_1}(k)] \times \mathcal{F} \times \mathcal{P}, \\
\mathcal{M}[V_8, B_8; P_8]_{1520} &= i^5 \int \frac{d^4 p}{(2\pi)^4} \frac{g_{VPP}}{\sqrt{2}} \frac{f_{\pi NN^*}^{1520}}{m_\pi} \bar{u}_\mu(p_4) \gamma_5 k^\mu (\not{p}_2 + m_2) [A_1 \gamma_\nu \gamma_5 + A_2 \frac{p_{2\nu}}{m_i} \\
&\quad \times \gamma_5 + B_1 \gamma_\nu + B_2 \frac{p_{2\nu}}{m_i}] \times u(p_i, s_i) \times \epsilon^{*\nu}(p_1) \epsilon^\alpha(p_1) (p_3 + k)_\alpha \times \mathcal{F} \\
&\quad \times \mathcal{P}, \\
\mathcal{M}[V_8, B_8; P_8]_{1535} &= -i^6 \int \frac{d^4 p}{(2\pi)^4} \frac{g_{VPP}}{\sqrt{2}} \frac{f_{\pi NN^*}^{1535}}{m_\pi} \bar{u}(p_4) \gamma_\mu k^\mu (\not{p}_2 + m_2) [A_1 \gamma_\nu \gamma_5 + A_2 \frac{p_{2\nu}}{m_i} \\
&\quad \times \gamma_5 + B_1 \gamma_\nu + B_2 \frac{p_{2\nu}}{m_i}] \times u(p_i, s_i) \times \epsilon^{*\nu}(p_1) \epsilon^\alpha(p_1) (p_3 + k)_\alpha \times \mathcal{F} \times \mathcal{P}, \\
\mathcal{M}[P_8, B_8; V_8]_{1520} &= i^8 \int \frac{d^4 p}{(2\pi)^4} \frac{g_{VPP}}{\sqrt{2}} \frac{g_{\rho NN^*}^{1520}}{m_\rho^2} \bar{u}_\kappa(p_4, s_4) \sigma_{\mu\nu} k^\nu k^\kappa (\not{p}_2 + m_2) [A + B \gamma_5] \\
&\quad \times u(p_i, s_i) \times \epsilon^{*\mu}(k) \epsilon^\alpha(k) (p_1 + p_3)_\alpha \times \mathcal{F} \times \mathcal{P}, 
\end{aligned} \tag{35}$$

$$\begin{aligned}
\mathcal{M}[P_8, B_8; V_8]_{1535} &= -i^6 \int \frac{d^4 p}{(2\pi)^4} \frac{g_{VPP}}{\sqrt{2}} \frac{g_{\rho NN^*}^{1535}}{m_\rho^2} \bar{u}(p_4, s_4) [\gamma_\mu(-k^2) - i(m_2 + m_4)k_\mu] \\
&\quad \times \gamma_5(\not{p}_2 + m_2) \times [A + B\gamma_5] u(p_i, s_i) \times \epsilon^{*\mu}(k) \epsilon^\alpha(k) (p_1 + p_3)_\alpha \\
&\quad \times \mathcal{F} \times \mathcal{P}, \\
\mathcal{M}[V_8, B_8; V_8]_{1520} &= -i^7 \int \frac{d^4 p}{(2\pi)^4} \frac{4g_{VVP}}{f_P} \frac{g_{\rho NN^*}^{1520}}{m_\rho^2} \bar{u}_\kappa(p_4, s_4) \sigma_{\mu\nu} k^\nu k^\kappa (\not{p}_2 + m_2) [A_1 \gamma_\alpha \gamma_5 \\
&\quad + A_2 \frac{p_{2\alpha}}{m_i} \gamma_5 + B_1 \gamma_\alpha + B_2 \frac{p_{2\alpha}}{m_i}] \times u(p_i, s_i) \epsilon_{\rho\sigma\beta\xi} p_1^\rho k^\beta \epsilon^{*\mu}(k) \epsilon^\xi(k) \\
&\quad \times \epsilon^{*\alpha}(p_1) \epsilon^\sigma(p_1) \times \mathcal{F} \times \mathcal{P}, \\
\mathcal{M}[V_8, B_8; V_8]_{1535} &= i^5 \int \frac{d^4 p}{(2\pi)^4} \frac{4g_{VVP}}{f_P} \frac{g_{\rho NN^*}^{1535}}{m_\rho^2} \bar{u}(p_4, s_4) [\gamma_\mu(-k^2) - i(m_2 + m_4)k_\mu] \gamma_5 \\
&\quad \times (\not{p}_2 + m_2) \times [A_1 \gamma_\nu \gamma_5 + A_2 \frac{p_{2\nu}}{m_i} \gamma_5 + B_1 \gamma_\nu + B_2 \frac{p_{2\nu}}{m_i}] u(p_i, s_i) \\
&\quad \times \epsilon_{\alpha\beta\rho\sigma} p_1^\alpha k^\rho \epsilon^{*\mu}(k) \epsilon^\sigma(k) \epsilon^{*\nu}(p_1) \times \epsilon^\beta(p_1) \times \mathcal{F} \times \mathcal{P}, \\
\mathcal{M}[V_8, B_8; B_8]_{1520} &= -i^4 \int \frac{d^4 p}{(2\pi)^4} \frac{2g_{PBB}}{\sqrt{6}} \frac{g_{\rho NN^*}^{1520}}{m_\rho^2} \bar{u}_\kappa(p_4, s_4) \sigma_{\mu\nu} p_1^\nu p_1^\kappa (\not{k} + m_k) \gamma_5 (\not{p}_2 \\
&\quad + m_2) [A_1 \gamma_\alpha \gamma_5 + A_2 \frac{p_{2\alpha}}{m_i} \gamma_5 + B_1 \gamma_\alpha + B_2 \frac{p_{2\alpha}}{m_i}] u(p_i, s_i) \epsilon^\mu(p_1) \\
&\quad \times \epsilon^{*\alpha}(p_1) \times \mathcal{F} \times \mathcal{P}, \tag{36} \\
\mathcal{M}[V_8, B_8; B_8]_{1535} &= i^4 \int \frac{d^4 p}{(2\pi)^4} \frac{2g_{PBB}}{\sqrt{6}} \frac{g_{\rho NN^*}^{1535}}{m_\rho^2} \bar{u}(p_4, s_4) [\gamma_\mu p_1^2 - i(m_k + m_4) p_{1\mu}] \\
&\quad \times \gamma_5(\not{k} + m_k) \gamma_5 \times (\not{p}_2 + m_2) [A_1 \gamma_\nu \gamma_5 + A_2 \frac{p_{2\nu}}{m_i} \gamma_5 + B_1 \gamma_\nu \\
&\quad + B_2 \frac{p_{2\nu}}{m_i}] u(p_i, s_i) \epsilon^\mu(p_1) \epsilon^{*\nu}(p_1) \times \mathcal{F} \times \mathcal{P}, \\
\mathcal{M}[P_8, B_8; B_8]_{1520} &= i^4 \int \frac{d^4 p}{(2\pi)^4} \frac{2g_{PBB}}{\sqrt{6}} \frac{f_{\pi NN^*}^{1520}}{m_\pi} \bar{u}_\mu(p_4, s_4) \gamma_5(\not{k} + m_k) \gamma_5 (\not{p}_2 + m_2) \\
&\quad \times [A + B\gamma_5] \times u(p_i, s_i) p_1^\mu \times \mathcal{F} \times \mathcal{P}, \\
\mathcal{M}[P_8, B_8; B_8]_{1535} &= -i^5 \int \frac{d^4 p}{(2\pi)^4} \frac{2g_{PBB}}{\sqrt{6}} \frac{f_{\pi NN^*}^{1535}}{m_\pi} \bar{u}(p_4, s_4) \gamma_\mu(\not{k} + m_k) \gamma_5 (\not{p}_2 + m_2) \\
&\quad \times [A + B\gamma_5] \times u(p_i, s_i) p_1^\mu \times \mathcal{F} \times \mathcal{P}.
\end{aligned}$$

The amplitudes of triangle diagrams for the decay  $\Lambda_b \rightarrow N^*(1520, 1535)V$ :

$$\begin{aligned}
\mathcal{M}[D, B_{\bar{3}}; D]_{1535} &= -i^7 \int \frac{d^4 p}{(2\pi)^4} g_{DDV} \frac{f_{D\bar{B}_3 N^*}^{1535}}{m_D} \bar{u}(p_4, s_4) \gamma_\mu k^\mu (\not{p}_2 + m_2) [A + B\gamma_5] \\
&\quad \times u(p_i, s_i) (k + p_1)_\nu \epsilon^{*\nu}(p_3) \times \mathcal{F} \times \mathcal{P}, \tag{37}
\end{aligned}$$

$$\begin{aligned}
\mathcal{M}[D, B_{\bar{3}}; D]_{1520} &= -i^6 \int \frac{d^4 p}{(2\pi)^4} g_{DDV} \frac{f_{DB_3 N^*}^{1520}}{m_D} \bar{u}_\mu(p_4, s_4) \gamma_5 k^\mu (\not{p}_2 + m_2) [A + B \gamma_5] \\
&\quad \times u(p_i, s_i) (k + p_1)_\nu \epsilon^{*\nu}(p_3) \times \mathcal{F} \times \mathcal{P}, \\
\mathcal{M}[D^*, B_{\bar{3}}; D]_{1535} &= -2i^6 \int \frac{d^4 p}{(2\pi)^4} f_{D^* DV} \frac{f_{DB_3 N^*}^{1535}}{m_D} \bar{u}(p_4, s_4) \gamma_\mu k^\mu (\not{p}_2 + m_2) [A_1 \gamma_\nu \gamma_5 \\
&\quad + A_2 \frac{p_{2\nu}}{m_i} \gamma_5 + B_1 \gamma_\nu + B_2 \frac{p_{2\nu}}{m_i}] \times u(p_i, s_i) \times \epsilon_{\alpha\beta\rho\sigma} p_3^\alpha (k + p_1)^\rho \epsilon^{*\beta}(p_3) \\
&\quad \times (-g^{\nu\sigma} + \frac{p_1^\nu p_1^\sigma}{p_1^2}) \times \mathcal{F} \times \mathcal{P}, \\
\mathcal{M}[D^*, B_{\bar{3}}; D]_{1520} &= -2i^5 \int \frac{d^4 p}{(2\pi)^4} f_{D^* DV} \frac{f_{DB_3 N^*}^{1520}}{m_\pi} \bar{u}_\mu(p_4, s_4) \gamma_5 k^\mu (\not{p}_2 + m_2) \\
&\quad \times [A_1 \gamma_\nu \gamma_5 + A_2 \frac{p_{2\nu}}{m_i} \gamma_5 + B_1 \gamma_\nu + B_2 \frac{p_{2\nu}}{m_i}] \times u(p_i, s_i) \times \epsilon_{\alpha\beta\rho\sigma} p_3^\alpha \epsilon^{*\beta}(p_3) \\
&\quad \times (p_1 + k)^\rho \times (-g^{\nu\sigma} + \frac{p_1^\nu p_1^\sigma}{p_1^2}) \times \mathcal{F} \times \mathcal{P}, \\
\mathcal{M}[D, B_{\bar{3}}; D^*]_{1535} &= -2i^5 \int \frac{d^4 p}{(2\pi)^4} f_{D^* DV} \frac{g_{D^* B_{\bar{3}} N^*}^{1535}}{m_{D^*}^2} \bar{u}(p_4, s_4) [\gamma_\mu k^2 - i(m_2 + m_4) k_\mu] \gamma_5 \\
&\quad \times (\not{p}_2 + m_2) \times [A + B \gamma_5] \times u(p_i, s_i) \epsilon_{\alpha\beta\rho\sigma} p_3^\alpha \epsilon^{*\beta}(p_3) (p_1 + k)^\rho \\
&\quad \times (-g^{\mu\sigma} + \frac{k^\mu k^\sigma}{k^2}) \times \mathcal{F} \times \mathcal{P}, \\
\mathcal{M}[D, B_{\bar{3}}; D^*]_{1520} &= 2i^7 \int \frac{d^4 p}{(2\pi)^4} f_{D^* DV} \frac{g_{D^* B_{\bar{3}} N^*}^{1520}}{m_{D^*}^2} \bar{u}_\kappa(p_4, s_4) \sigma_{\mu\nu} k^\nu k^\kappa (\not{p}_2 + m_2) [A \\
&\quad + B \gamma_5] \times u(p_i, s_i) \epsilon_{\alpha\beta\rho\sigma} p_3^\alpha \epsilon^{*\beta}(p_3) (p_1 + k)^\rho (-g^{\mu\sigma} + \frac{k^\mu k^\sigma}{k^2}) \\
&\quad \times \mathcal{F} \times \mathcal{P}, \\
\mathcal{M}[D^*, B_{\bar{3}}; D^*]_{1535} &= -i^4 \int \frac{d^4 p}{(2\pi)^4} \frac{g_{D^* B_{\bar{3}} N^*}^{1535}}{m_{D^*}^2} \bar{u}(p_4, s_4) [\gamma_\mu k^2 - i(m_2 + m_4) k_\mu] \gamma_5 (\not{p}_2 \\
&\quad + m_2) [A_1 \gamma^\nu \gamma_5 + A_2 \frac{p_2^\nu}{m_i} \gamma_5 + B_1 \gamma^\nu + B_2 \frac{p_2^\nu}{m_i}] u(p_i, s_i) \epsilon^\mu(k) \epsilon^{*\nu}(p_1) \\
&\quad \times \{g_{D^* D^* V}(k + p_1)_\alpha \epsilon^{*\beta}(k) \epsilon_\beta(p_1) \epsilon^{*\alpha}(p_3) + 4f_{D^* D^* V} \epsilon_\alpha^*(k) [p_3^\alpha \epsilon^{*\beta}(p_3) \\
&\quad - p_3^\beta \epsilon^{*\alpha}(p_3)] \epsilon_\beta(p_1)\} \times \mathcal{F} \times \mathcal{P}, \\
\mathcal{M}[D^*, B_{\bar{3}}; D^*]_{1520} &= i^2 \int \frac{d^4 p}{(2\pi)^4} \frac{g_{D^* B_{\bar{3}} N^*}^{1520}}{m_{D^*}^2} \bar{u}_\kappa(p_4, s_4) \sigma_{\mu\nu} k^\nu k^\kappa (\not{p}_2 + m_2) [A_1 \gamma^\alpha \gamma_5 \\
&\quad + A_2 \frac{p_2^\alpha}{m_i} \gamma_5 + B_1 \gamma^\alpha + B_2 \frac{p_2^\alpha}{m_i}] u(p_i, s_i) \epsilon^\mu(k) \epsilon^{*\alpha}(p_1) \{g_{D^* D^* V}(k + p_1)_\rho \\
&\quad \times \epsilon^{*\sigma}(k) \epsilon_\sigma(p_1) \epsilon^\rho(p_3) + 4f_{D^* D^* V} \epsilon_\rho^*(k) [p_3^\rho \epsilon^{*\sigma}(p_3) - p_3^\sigma \epsilon^{*\rho}(p_3)] \\
&\quad \times \epsilon_\sigma(p_1)\} \times \mathcal{F} \times \mathcal{P}, \\
\mathcal{M}[P_8, B_8; P_8]_{1535} &= -i^7 \int \frac{d^4 p}{(2\pi)^4} \frac{g_{VPP}}{\sqrt{2}} \frac{f_{\pi N N^*}^{1535}}{m_\pi} \bar{u}(p_4, s_4) \gamma_\mu k^\mu (\not{p}_2 + m_2) [A + B \gamma_5] \\
&\quad \times u(p_i, s_i) \times (p_1 - k)_\nu \epsilon^{*\nu}(p_3) \times \mathcal{F} \times \mathcal{P}, \tag{38}
\end{aligned}$$

$$\begin{aligned}
\mathcal{M}[P_8, B_8; P_8]_{1520} &= i^6 \int \frac{d^4 p}{(2\pi)^4} \frac{g_{VPP}}{\sqrt{2}} \frac{f_{\pi NN^*}^{1520}}{m_\pi} \bar{u}_\mu(p_4, s_4) \gamma_5 k^\mu (\not{p}_2 + m_2) [A + B \gamma_5] \\
&\quad \times u(p_i, s_i) \times (p_1 - k)_\nu \epsilon^{*\nu}(p_3) \times \mathcal{F} \times \mathcal{P}, \\
\mathcal{M}[V_8, B_8; P_8]_{1535} &= -i^6 \int \frac{d^4 p}{(2\pi)^4} \frac{4g_{VVP}}{f_P} \frac{f_{\pi NN^*}^{1535}}{m_\pi} \bar{u}(p_4, s_4) \gamma_\mu k^\mu (\not{p}_2 + m_2) [A_1 \gamma_\nu \gamma_5 \\
&\quad + A_2 \frac{p_{2\nu}}{m_i} \gamma_5 + B_1 \gamma_\nu + B_2 \frac{p_{2\nu}}{m_i}] \times u(p_i, s_i) \epsilon_{\alpha\beta\rho\sigma} p_3^\alpha p_1^\rho \epsilon^{*\beta}(p_3) \\
&\quad \times \epsilon^\sigma(p_1) \epsilon^{*\nu}(p_1) \times \mathcal{F} \times \mathcal{P}, \\
\mathcal{M}[V_8, B_8; P_8]_{1520} &= -i^5 \int \frac{d^4 p}{(2\pi)^4} \frac{4g_{VVP}}{f_P} \frac{f_{\pi NN^*}^{1520}}{m_\pi} \bar{u}_\mu(p_4, s_4) \gamma_5 k^\mu (\not{p}_2 + m_2) [A_1 \gamma_\nu \gamma_5 \\
&\quad + A_2 \frac{p_{2\nu}}{m_i} \gamma_5 + B_1 \gamma_\nu + B_2 \frac{p_{2\nu}}{m_i}] \times u(p_i, s_i) \epsilon_{\alpha\beta\rho\sigma} p_3^\alpha p_1^\rho \epsilon^{*\beta}(p_3) \epsilon^\sigma(p_1) \\
&\quad \times \epsilon^{*\nu}(p_1) \times \mathcal{F} \times \mathcal{P}, \\
\mathcal{M}[P_8, B_8; V_8]_{1535} &= -i^6 \int \frac{d^4 p}{(2\pi)^4} \frac{4g_{VVP}}{f_P} \frac{g_{\rho NN^*}^{1535}}{m_\rho} \bar{u}(p_4, s_4) [\gamma_\mu(-k^2) - i(m_2 + m_4) k_\mu] \\
&\quad \times \gamma_5 (\not{p}_2 + m_2) \times [A + B \gamma_5] u(p_i, s_i) \times \epsilon_{\alpha\beta\rho\sigma} k^\alpha p_3^\rho \epsilon^{*\sigma}(p_3) \epsilon^{*\mu}(k) \\
&\quad \times \epsilon^\beta(k) \times \mathcal{F} \times \mathcal{P}, \\
\mathcal{M}[P_8, B_8; V_8]_{1520} &= -i^6 \int \frac{d^4 p}{(2\pi)^4} \frac{4g_{VVP}}{f_P} \frac{g_{\rho NN^*}^{1520}}{m_\rho} \bar{u}_\kappa(p_4, s_4) \sigma_{\mu\nu} k^\nu k^\kappa (\not{p}_2 + m_2) [A + B \gamma_5] \\
&\quad \times u(p_i, s_i) \times \epsilon_{\alpha\beta\rho\sigma} k^\alpha p_3^\rho \epsilon^{*\sigma}(p_3) \epsilon^{*\mu}(k) \epsilon^\beta(k) \times \mathcal{F} \times \mathcal{P}, \\
\mathcal{M}[V_8, B_8; V_8]_{1535} &= -i^5 \int \frac{d^4 p}{(2\pi)^4} \frac{g_{VVP}}{\sqrt{2}} \frac{g_{\rho NN^*}^{1535}}{m_\rho^2} \bar{u}(p_4, s_4) [\gamma_\mu k^2 + i(m_2 + m_4) k_\mu] \gamma_5 (\not{p}_2 \\
&\quad + m_2) [A_1 \gamma_\nu \gamma_5 + A_2 \frac{p_{2\nu}}{m_i} \gamma_5 + B_1 \gamma_\nu + B_2 \frac{p_{2\nu}}{m_i}] u(p_i, s_i) \epsilon^{*\nu}(p_1) \epsilon^{*\mu}(k) \\
&\quad \times [-k_\beta \epsilon_\alpha(k) \epsilon^{*\alpha}(p_3) \epsilon^\beta(p_1) - \epsilon_\alpha(k) p_{3\beta} \epsilon^{*\alpha}(p_3) \epsilon^\beta(p_1) + p_{3\beta} \epsilon_\alpha^*(p_3) \\
&\quad \times \epsilon^\alpha(p_1) \epsilon^\beta(k) + \epsilon^{*\alpha}(p_3) p_{1\beta} \epsilon_\alpha(p_1) \epsilon^\beta(k)] \times \mathcal{F} \times \mathcal{P}, \\
\mathcal{M}[V_8, B_8; V_8]_{1520} &= i^5 \int \frac{d^4 p}{(2\pi)^4} \frac{g_{VVP}}{\sqrt{2}} \frac{g_{\rho NN^*}^{1520}}{m_\rho^2} \bar{u}_\kappa(p_4, s_4) \sigma_{\mu\nu} k^\nu k^\kappa (\not{p}_2 + m_2) [A_1 \gamma_\xi \gamma_5 \\
&\quad + A_2 \frac{p_{2\xi}}{m_i} \gamma_5 + B_1 \gamma_\xi + B_2 \frac{p_{2\xi}}{m_i}] \times u(p_i, s_i) \epsilon^{*\mu}(k) \epsilon^{*\xi}(p_1) [-k_\beta \epsilon_\alpha(k) \\
&\quad \times \epsilon^{*\alpha}(p_3) \epsilon^\beta(p_1) - \epsilon_\alpha(k) p_{3\beta} \epsilon^{*\alpha}(p_3) \epsilon^\beta(p_1) + p_{3\beta} \epsilon_\alpha^*(p_3) \epsilon^\alpha(p_1) \epsilon^\beta(k) \\
&\quad + \epsilon^{*\alpha}(p_3) p_{1\beta} \epsilon_\alpha(p_1) \epsilon^\beta(k)] \times \mathcal{F} \times \mathcal{P}. \tag{39}
\end{aligned}$$

The amplitude of triangle diagrams for the decay  $\Lambda_b \rightarrow N^*(1535, 1520)S$  are

$$\begin{aligned}
\mathcal{M}[D, B_{\bar{3}}; D]_{1520} &= -i^5 \int \frac{d^4 k}{(2\pi)^4} \frac{\gamma_{\sigma DD}}{\sqrt{2}} \frac{f_{DB_{\bar{3}}N^*}^{1520}}{m_D} \bar{u}_\mu(p_4, s_4) \gamma_5 k^\mu (\not{p}_2 + m_2) [A + B \gamma_5] \\
&\quad \times u(p_i, s_i) p_{1\nu} k^\nu \mathcal{F} \times \mathcal{P}, \tag{40}
\end{aligned}$$

$$\begin{aligned}
\mathcal{M}[D, B_{\bar{3}}; D]_{1535} &= i^6 \int \frac{d^4 k}{(2\pi)^4} \frac{\gamma_{\sigma DD}}{\sqrt{2}} \frac{f_{DB_{\bar{3}}N^*}^{1535}}{m_D} \bar{u}_\mu(p_4, s_4) \gamma_\mu k^\mu (\not{p}_2 + m_2) [A + B\gamma_5] \\
&\quad \times u(p_i, s_i) p_{1\nu} k^\nu \mathcal{F} \times \mathcal{P}, \\
\mathcal{M}[D, B_{\bar{3}}; B_{\bar{3}}]_{1520} &= -i^4 \int \frac{d^4 p}{(2\pi)^4} \frac{f_{DB_{\bar{3}}N^*}^{1520}}{m_D} g_{\sigma NN} \bar{u}_\mu(p_4, s_4) \gamma_5 p_1^\mu (\not{k} + m_k) (\not{p}_2 + m_2) \\
&\quad \times [A + B\gamma_5] \times u(p_i, s_i) \times \mathcal{F} \times \mathcal{P}, \\
\mathcal{M}[D, B_{\bar{3}}; B_{\bar{3}}]_{1535} &= i^5 \int \frac{d^4 p}{(2\pi)^4} \frac{f_{DB_{\bar{3}}N^*}^{1520}}{m_D} g_{\sigma NN} \bar{u}(p_4, s_4) \gamma_\mu p_1^\mu (\not{k} + m_k) (\not{p}_2 + m_2) [A \\
&\quad + B\gamma_5] \times u(p_i, s_i) \times \mathcal{F} \times \mathcal{P}, \\
\mathcal{M}[D^*, B_{\bar{3}}; B_{\bar{3}}]_{1520} &= i^5 \int \frac{d^4 p}{(2\pi)^4} \frac{g_{D^*B_{\bar{3}}N^*}^{1520}}{m_{D^*}^2} g_{\sigma NN} \bar{u}_\kappa(p_4, s_4) \sigma_{\mu\nu} p_1^\nu p_1^\kappa (\not{k} + m_k) (\not{p}_2 \\
&\quad + m_2) [A_1 \gamma_\alpha \gamma_5 + A_2 \frac{p_{2\alpha}}{m_i} \gamma_5 + B_1 \gamma_\alpha + B_2 \frac{p_{2\alpha}}{m_i}] u(p_i, s_i) \epsilon^\mu(p_1) \epsilon^{*\alpha}(p_1) \\
&\quad \times \mathcal{F} \times \mathcal{P}, \\
\mathcal{M}[D^*, B_{\bar{3}}; B_{\bar{3}}]_{1535} &= -i^3 \int \frac{d^4 p}{(2\pi)^4} \frac{g_{D^*B_{\bar{3}}N^*}^{1520}}{m_{D^*}^2} g_{\sigma NN} \bar{u}(p_4, s_4) [\gamma_\mu p_1^2 + i(m_4 + m_k) p_{1\mu}] \\
&\quad \gamma_5 (\not{k} + m_k) \times (\not{p}_2 + m_2) [A_1 \gamma_\alpha \gamma_5 + A_2 \frac{p_{2\alpha}}{m_i} \gamma_5 + B_1 \gamma_\alpha + B_2 \frac{p_{2\alpha}}{m_i}] u(p_i, s_i) \\
&\quad \times \epsilon^\mu(p_1) \epsilon^{*\alpha}(p_1) \times \mathcal{F} \times \mathcal{P}, \\
\mathcal{M}[P_8, B_8; P_8]_{1520} &= -\sqrt{2} i^6 \int \frac{d^4 p}{(2\pi)^4} \gamma_{\sigma\pi\pi} \frac{f_{\pi NN^*}^{1520}}{m_\pi} \epsilon^{*\mu}(p_4) \bar{u}(p_4, s_4) \gamma_5 k_\mu (\not{p}_2 + m_2) [A \\
&\quad + B\gamma_5] u(p_i, s_i) p_{1\nu} k^\nu \times \mathcal{F} \times \mathcal{P}, \\
\mathcal{M}[P_8, B_8; P_8]_{1535} &= -\sqrt{2} i^7 \int \frac{d^4 p}{(2\pi)^4} \gamma_{\sigma\pi\pi} \frac{f_{\pi NN^*}^{1535}}{m_\pi} \bar{u}(p_4, s_4) \gamma^\mu k_\mu (\not{p}_2 + m_2) [A + B\gamma_5] \\
&\quad \times u(p_i, s_i) p_{1\nu} k^\nu \times \mathcal{F} \times \mathcal{P}, \\
\mathcal{M}[P_8, B_8; B_8]_{1520} &= i^4 \int \frac{d^4 p}{(2\pi)^4} g_{\sigma NN} \frac{f_{\pi NN^*}^{1520}}{m_\pi} \epsilon^{*\mu}(p_4) \bar{u}(p_4, s_4) \gamma_5 p_{1\mu} (\not{k} + m_k) (\not{p}_2 \\
&\quad + m_2) \times [A + B\gamma_5] \times u(p_i, s_i) \times \mathcal{F} \times \mathcal{P}, \\
\mathcal{M}[P_8, B_8; B_8]_{1535} &= i^5 \int \frac{d^4 p}{(2\pi)^4} g_{\sigma NN} \frac{f_{\pi NN^*}^{1535}}{m_\pi} \bar{u}(p_4, s_4) \gamma^\mu p_{1\mu} (\not{k} + m_k) (\not{p}_2 + m_2) [A \\
&\quad + B\gamma_5] u(p_i, s_i) \times \mathcal{F} \times \mathcal{P}, \\
\mathcal{M}[V_8, B_8; B_8]_{1520} &= i^5 \int \frac{d^4 p}{(2\pi)^4} g_{\sigma NN} \frac{g_{\rho NN^*}^{1520}}{m_\rho^2} \bar{u}_\alpha(p_4, s_4) \sigma_{\mu\nu} p_1^\nu p_1^\alpha \epsilon^{*\mu}(p_1) (\not{k} + m_k) (\not{p}_2 \\
&\quad + m_2) \epsilon^{*\beta}(p_1) [A_1 \gamma_\beta \gamma_5 + A_2 \frac{p_{2\beta}}{m_i} \gamma_5 + B_1 \gamma_\beta + B_2 \frac{p_{2\beta}}{m_i}] u(p_i, s_i) \times \mathcal{F} \\
&\quad \times \mathcal{P}, \tag{41}
\end{aligned}$$

$$\begin{aligned}
\mathcal{M}[V_8, B_8; B_8]_{1535} = & -i^3 \int \frac{d^4 p}{(2\pi)^4} g_{\sigma NN} \frac{g_{\rho NN}^{1535}}{m_\rho^2} \bar{u}(p_4, s_4) [\gamma_\mu k^2 - i(m_2 + m_k)p_{1\mu}] \gamma_5 \\
& \times \epsilon^{*\mu}(p_1) (\not{k} + m_k) \times (\not{p}_2 + m_2) \epsilon^{*\beta}(p_1) [A_1 \gamma_\beta \gamma_5 + A_2 \frac{p_{2\beta}}{m_i} \gamma_5 + B_1 \gamma_\beta \\
& + B_2 \frac{p_{2\beta}}{m_i}] u(p_i, s_i) \times \mathcal{F} \times \mathcal{P}, \tag{42}
\end{aligned}$$

where  $P_8, V_8, B_8, B_{\bar{3}}$  and  $S$  denote pseudoscalar meson octet, vector meson octet, baryon octet, anti-triplets and scalar mesons.

## D Full expressions of amplitudes

We present the expressions for the full amplitudes of  $\Lambda_b$  decay channels

- $\Lambda_b \rightarrow N_{1520,1535}^* K_S$ :

$$\begin{aligned}
\mathcal{A}(\Lambda_b \rightarrow N_{1520,1535}^* K_S) = & \mathcal{S}(\Lambda_b \rightarrow N^* K_S) + \mathcal{M}[D_s^{*-}, \Lambda_c^+; D^-] + \mathcal{M}[D_s^-, \Lambda_c^+; D^{*-}] \\
& + \mathcal{M}[D_s^-, \Lambda_c^+; D^{*-}] + \mathcal{M}[K^{*-}, p; \pi^+] + \mathcal{M}[K^-, p; \rho^+] + \mathcal{M}[K^{*-}, p; \rho^+] \\
& + \mathcal{M}[\bar{K}^{*0}, n; \pi^0] + \mathcal{M}[\bar{K}^{*0}, n; \rho^0] + \mathcal{M}[\bar{K}^{*0}, n; \omega] + \mathcal{M}[\bar{K}^0, n; \rho^0] \\
& + \mathcal{M}[\bar{K}^0, n; \omega] + \mathcal{M}[\rho^0, \Lambda^0; \bar{K}^0] + \mathcal{M}[\omega, \Lambda^0; \bar{K}^0] + \mathcal{M}[\phi, \Lambda^0; \bar{K}^{*0}] \\
& + \mathcal{M}[\pi^0, \Lambda^0; \bar{K}^{*0}] + \mathcal{M}[\rho^0, \Lambda^0; n] + \mathcal{M}[\omega, \Lambda^0; n] + \mathcal{M}[\pi^0, \Lambda^0; n]. \tag{43}
\end{aligned}$$

- $\Lambda_b \rightarrow N_{1520,1535}^* \bar{K}^{*0}$ :

$$\begin{aligned}
\mathcal{A}(\Lambda_b \rightarrow N_{1520,1535}^* \bar{K}^{*0}) = & \mathcal{S}(\Lambda_b \rightarrow N^* \bar{K}^{*0}) + \mathcal{M}[D_s^-, \Lambda_c^+; D^-] + \mathcal{M}[D_s^{*-}, \Lambda_c^+; D^-] \\
& + \mathcal{M}[D_s^-, \Lambda_c^+; D^{*-}] + \mathcal{M}[D_s^{*-}, \Lambda_c^+; D^{*-}] + \mathcal{M}[K^-, p; \pi^+] + \mathcal{M}[K^-, p; \rho^+] \\
& + \mathcal{M}[K^{*-}, p; \rho^+] + \mathcal{M}[K^{*-}, p; \pi^+] + \mathcal{M}[\bar{K}^0, n; \pi^0] + \mathcal{M}[\bar{K}^0, n; \rho^0] \\
& + \mathcal{M}[\bar{K}^0, n; \omega] + \mathcal{M}[\bar{K}^{*0}, n; \pi^0] + \mathcal{M}[\bar{K}^{*0}, n; \rho^0] + \mathcal{M}[\bar{K}^{*0}, n; \omega] \\
& + \mathcal{M}[\pi^0, \Lambda^0; \bar{K}^0] + \mathcal{M}[\rho^0, \Lambda^0; \bar{K}^0] + \mathcal{M}[\omega, \Lambda^0; \bar{K}^0] + \mathcal{M}[\phi, \Lambda^0; \bar{K}^0] \\
& + \mathcal{M}[\pi^0, \Lambda^0; \bar{K}^{*0}] + \mathcal{M}[\rho^0, \Lambda^0; \bar{K}^{*0}] + \mathcal{M}[\omega, \Lambda^0; \bar{K}^{*0}] + \mathcal{M}[\phi, \Lambda^0; \bar{K}^{*0}]. \tag{44}
\end{aligned}$$

- $\Lambda_b \rightarrow N_{1520,1535}^* K_0^*(700)$ :

$$\begin{aligned}
\mathcal{A}(\Lambda_b \rightarrow N_{1520,1535}^* K_0^*(700)) = & \mathcal{S}(\Lambda_b \rightarrow N^* K_0^*(700)) + \mathcal{M}[D_s^-, \Lambda_c^+; D^-] \\
& + \mathcal{M}[K^-, p; \pi^+] + \mathcal{M}[\bar{K}^0, n; \pi^0] + \mathcal{M}[\pi^0, \Lambda^0; \bar{K}^0] + \mathcal{M}[\pi^0, \Lambda^0; n] \\
& + \mathcal{M}[\rho^0, \Lambda^0; n] + \mathcal{M}[\omega, \Lambda^0; n]. \tag{45}
\end{aligned}$$

- $\Lambda_b \rightarrow N_{1520,1535}^* f_0(500, 980)$ :

$$\begin{aligned}
\mathcal{A}(\Lambda_b \rightarrow N_{1520,1535}^* f_0(500, 980)) = & \mathcal{S}(\Lambda_b \rightarrow N^* f_0(500, 980)) + \mathcal{M}[D^-, \Lambda_c^+; D^+] \\
& + \mathcal{M}[D^-, \Lambda_c^+; \Lambda_c^+] + \mathcal{M}[D^{*-}, \Lambda_c^+; \Lambda_c^+] + \mathcal{M}[\pi^-, p; \pi^+] + \mathcal{M}[\pi^-, p; p] \\
& + \mathcal{M}[\rho^-, p; p] + \mathcal{M}[\pi^0, n; \pi^0] + \mathcal{M}[\pi^0, n; n] + \mathcal{M}[\rho^0, n; n] + \mathcal{M}[\omega, n; n] \\
& + \mathcal{M}[K^0, \Lambda^0; \bar{K}^0] + \mathcal{M}[K^0, \Lambda^0; \Lambda^0] + \mathcal{M}[K^{*0}, \Lambda^0; \Lambda^0]. \tag{46}
\end{aligned}$$

- $\Lambda_b \rightarrow N_{1520,1535}^* \rho^0(770)$  :

$$\begin{aligned}
\mathcal{A}(\Lambda_b \rightarrow N_{1520,1535}^* \rho^0(770)) = & \mathcal{S}(\Lambda_b \rightarrow N^* \rho^0(770)) + \mathcal{M}[D^-, \Lambda_c^+; D^-] \\
& + \mathcal{M}[D^-, \Lambda_c^+; D^{*-}] + \mathcal{M}[D^{*-}, \Lambda_c^+; D^-] + \mathcal{M}[D^{*-}, \Lambda_c^+; D^{*-}] \\
& + \mathcal{M}[D^-, \Lambda_c^+; \Sigma_c^+] + \mathcal{M}[D^{*-}, \Lambda_c^+; \Sigma_c^+] + \mathcal{M}[\pi^-, p; \pi^+] \\
& + \mathcal{M}[\rho^-, p; \rho^+] + \mathcal{M}[\pi^-, p; p] + \mathcal{M}[\rho^-, p; p] + \mathcal{M}[\omega, n; \pi^0] \\
& + \mathcal{M}[\pi^0, n; \omega] + \mathcal{M}[\pi^0, n; n] + \mathcal{M}[\rho^0, n; n] + \mathcal{M}[\omega, n; n] \\
& + \mathcal{M}[K^0, \Lambda^0; \bar{K}^0] + \mathcal{M}[K^0, \Lambda^0; \bar{K}^{*0}] + \mathcal{M}[K^{*0}, \Lambda^0; \bar{K}^0] \\
& + \mathcal{M}[K^{*0}, \Lambda^0; \bar{K}^{*0}] .
\end{aligned} \tag{47}$$

- $\Lambda_b \rightarrow N_{1520,1535}^* \phi$  :

$$\begin{aligned}
\mathcal{A}(\Lambda_b \rightarrow N_{1520,1535}^* \phi) = & \mathcal{S}(\Lambda_b \rightarrow N^* \phi) + \mathcal{M}[K^0, \Lambda^0; \bar{K}^0] + \mathcal{M}[K^0, \Lambda^0; \bar{K}^{*0}] \\
& + \mathcal{M}[K^{*0}, \Lambda^0; \bar{K}^0] + \mathcal{M}[K^{*0}, \Lambda^0; \bar{K}^{*0}] + \mathcal{M}[K^0, \Lambda^0; \Lambda^0] + \mathcal{M}[K^{*0}, \Lambda^0; \Lambda^0],
\end{aligned} \tag{48}$$

where  $\mathcal{S}$  denotes the short-distance contributions.

## References

- [1] A. D. Sakharov, Pisma Zh. Eksp. Teor. Fiz. **5**, 32 (1967).
- [2] N. Cabibbo, Phys. Rev. Lett. **10**, 531 (1963).
- [3] M. Kobayashi and T. Maskawa, Prog. Theor. Phys. **49**, 652 (1973).
- [4] P. A. R. Ade et al. (Planck), Astron. Astrophys. **594**, A13 (2016), arXiv:1502.01589 [astro-ph.CO].
- [5] F. Muller, R. W. Birge, W. B. Fowler, R. H. Good, W. Hirsch, R. P. Matsen, L. Oswald, W. M. Powell, H. S. White, and O. Piccioni, Phys. Rev. Lett. **4**, 418 (1960).
- [6] J. H. Christenson, J. W. Cronin, V. L. Fitch, and R. Turlay, Phys. Rev. Lett. **13**, 138 (1964).
- [7] A. Alavi-Harati et al. (KTeV), Phys. Rev. Lett. **83**, 22 (1999), arXiv:hep-ex/9905060 .
- [8] B. Aubert et al. (BaBar), Phys. Rev. Lett. **86**, 2515 (2001), arXiv:hep-ex/0102030 .
- [9] K. Abe et al. (Belle), Phys. Rev. Lett. **87**, 091802 (2001), arXiv:hep-ex/0107061 .
- [10] B. Aubert et al. (BaBar), Phys. Rev. Lett. **93**, 131801 (2004), arXiv:hep-ex/0407057 .
- [11] Y. Chao et al. (Belle), Phys. Rev. Lett. **93**, 191802 (2004), arXiv:hep-ex/0408100 .
- [12] R. Aaij et al. (LHCb), Phys. Rev. Lett. **110**, 221601 (2013), arXiv:1304.6173 [hep-ex] .

- [13] R. Aaij et al. (LHCb), Phys. Rev. Lett. **122**, 211803 (2019), arXiv:1903.08726 [hep-ex] .
- [14] R. Aaij et al. (LHCb), Nature **643**, 1223 (2025), arXiv:2503.16954 [hep-ex] .
- [15] H.-Y. Cheng, C.-K. Chua, and A. Soni, Physical Review D **71** (2005), 10.1103/physrevd.71.014030.
- [16] C.-P. Jia, H.-Y. Jiang, J.-P. Wang, and F.-S. Yu, JHEP **11**, 072 (2024), arXiv:2408.14959 [hep-ph] .
- [17] G. Buchalla, A. J. Buras, and M. E. Lautenbacher, Rev. Mod. Phys. **68**, 1125 (1996), arXiv:hep-ph/9512380 .
- [18] C.-D. Lu, Y.-M. Wang, H. Zou, A. Ali, and G. Kramer, Phys. Rev. D **80**, 034011 (2009), arXiv:0906.1479 [hep-ph] .
- [19] D. Fakirov and B. Stech, Nucl. Phys. B **133**, 315 (1978).
- [20] T. D. Lee and C.-N. Yang, Phys. Rev. **108**, 1645 (1957).
- [21] S. Pakvasa, S. P. Rosen, and S. F. Tuan, Phys. Rev. D **42**, 3746 (1990).
- [22] J. Zhu, Z.-T. Wei, and H.-W. Ke, Phys. Rev. D **99**, 054020 (2019), arXiv:1803.01297 [hep-ph] .
- [23] L. Wolfenstein, Phys. Rev. D **43**, 151 (1991).
- [24] M. Suzuki and L. Wolfenstein, Phys. Rev. D **60**, 074019 (1999), arXiv:hep-ph/9903477 .
- [25] H.-Y. Cheng, C.-K. Chua, and A. Soni, Phys. Rev. D **71**, 014030 (2005), arXiv:hep-ph/0409317 .
- [26] H.-Y. Cheng and C.-K. Chua, Phys. Rev. D **102**, 053006 (2020), arXiv:2007.02558 [hep-ph] .
- [27] P. C. Magalhaes, M. R. Robilotta, K. S. F. F. Guimaraes, T. Frederico, W. de Paula, I. Bediaga, A. C. d. Reis, C. M. Maekawa, and G. R. S. Zarnauskas, Phys. Rev. D **84**, 094001 (2011), arXiv:1105.5120 [hep-ph] .
- [28] R. A. Garrote, J. Cuervo, P. C. Magalhães, and J. R. Peláez, Phys. Rev. Lett. **130**, 201901 (2023), arXiv:2210.08354 [hep-ph] .
- [29] Z.-L. Yue, Q.-Y. Guo, and D.-Y. Chen, Phys. Rev. D **109**, 094049 (2024), arXiv:2402.10594 [hep-ph] .
- [30] Z.-D. Duan, J.-P. Wang, R.-H. Li, C.-D. Lv, and F.-S. Yu, (2024), arXiv:2412.20458 [hep-ph] .
- [31] R. L. Workman et al. (Particle Data Group), PTEP **2022**, 083C01 (2022).
- [32] H.-W. Ke, X.-Q. Li, and Z.-T. Wei, Phys. Rev. D **77**, 014020 (2008), arXiv:0710.1927 [hep-ph] .

- [33] Z.-T. Wei, H.-W. Ke, and X.-Q. Li, Phys. Rev. D **80**, 094016 (2009), arXiv:0909.0100 [hep-ph] .
- [34] J. Zhu, H.-W. Ke, and Z.-T. Wei, Eur. Phys. J. C **76**, 284 (2016), arXiv:1603.02800 [hep-ph] .
- [35] T. Feldmann and M. W. Y. Yip, Phys. Rev. D **85**, 014035 (2012), [Erratum: Phys. Rev. D 86, 079901 (2012)], arXiv:1111.1844 [hep-ph] .
- [36] A. Khodjamirian, C. Klein, T. Mannel, and Y.-M. Wang, Journal of High Energy Physics **2011** (2011), 10.1007/jhep09(2011)106.
- [37] T. M. Aliev, A. Ozpineci, S. B. Yakovlev, and V. Zamiralov, Phys. Rev. D **74**, 116001 (2006).
- [38] T. M. Aliev, A. Ozpineci, M. Savci, and V. S. Zamiralov, Phys. Rev. D **80**, 016010 (2009), arXiv:0905.4664 [hep-ph] .
- [39] D. O. Riska and G. E. Brown, Nucl. Phys. A **679**, 577 (2001), arXiv:nucl-th/0005049 .
- [40] Z.-L. Yue, Q.-Y. Guo, and D.-Y. Chen, “Strong decays of the  $\lambda_c(2910)$  and  $\lambda_c(2940)$  in the  $nd^*$  molecular frame,” (2024), arXiv:2402.10594 [hep-ph] .
- [41] F.-S. Yu, H.-Y. Jiang, R.-H. Li, C.-D. Lü, W. Wang, and Z.-X. Zhao, Chin. Phys. C **42**, 051001 (2018), arXiv:1703.09086 [hep-ph] .
- [42] S. Okubo, Physics Letters **5**, 165 (1963).
- [43] H. Chen and R.-G. Ping, Phys. Rev. D **99**, 114027 (2019).
- [44] S. Roy, R. Sinha, and N. G. Deshpande, Phys. Rev. D **101**, 036018 (2020), arXiv:1911.01121 [hep-ph] .
- [45] F. Giacosa and G. Pagliara, Nucl. Phys. A **833**, 138 (2010), arXiv:0905.3706 [hep-ph] .
- [46] S. Navas et al. (Particle Data Group), Phys. Rev. D **110**, 030001 (2024).
- [47] J.-J. Han, J.-X. Yu, Y. Li, H.-n. Li, J.-P. Wang, Z.-J. Xiao, and F.-S. Yu, Phys. Rev. Lett. **134**, 221801 (2025), arXiv:2409.02821 [hep-ph] .
- [48] P.-C. Hong, F. Yan, R.-G. Ping, and T. Luo, Chin. Phys. C **47**, 053101 (2023), arXiv:2211.16014 [hep-ph] .
- [49] J. F. Donoghue, X.-G. He, and S. Pakvasa, Phys. Rev. D **34**, 833 (1986).
- [50] J.-J. Qi, Z.-Y. Wang, Z.-H. Zhang, and X.-H. Guo, (2025), arXiv:2511.12445 [hep-ph] .
- [51] J.-P. Wang and F.-S. Yu, Phys. Lett. B **849**, 138460 (2024), arXiv:2208.01589 [hep-ph] .
- [52] J. W. Cronin and O. E. Overseth, Phys. Rev. **129**, 1795 (1963).

- [53] O. E. Overseth and R. F. Roth, Phys. Rev. Lett. **19**, 391 (1967).
- [54] C. Q. Geng and C.-W. Liu, Phys. Lett. B **825**, 136883 (2022), arXiv:2106.10628 [hep-ph] .
- [55] J.-P. Wang, Q. Qin, and F.-S. Yu, (2024), arXiv:2411.18323 [hep-ph] .